

Higher Quarkonia

T.Barnes,^{1*} F.E.Close,² P.R.Page,³ E.S.Swanson⁴

¹*Theoretical and Computational Physics Section, Oak Ridge National Laboratory,*

Oak Ridge, TN 37831-6373, USA

Department of Physics and Astronomy, University of Tennessee,

Knoxville, TN 37996-1501, USA

²*Particle Theory, Rutherford-Appleton Laboratory, Chilton, Didcot OX11 0QX, UK*

³*Department of Physics and Astronomy, University of Manchester, Manchester M13 9PL, UK*

⁴*Department of Physics, North Carolina State University, Raleigh, NC 27695-8202, USA*

(September 1996)

Abstract

We discriminate gluonic hadrons from conventional $q\bar{q}$ states by surveying radial and orbital excitations of all $I=0$ and $I=1$ $n\bar{n}$ systems anticipated up to 2.1 GeV. We give detailed predictions of their quasi-two-body branching fractions and identify characteristic decay modes that can isolate quarkonia. Several of the “missing mesons” with $L_{q\bar{q}} = 2$ and $L_{q\bar{q}} = 3$ are predicted to decay dominantly into certain S+P and S+D modes, and should appear in experimental searches for hybrids in the same mass region. We also consider the topical issues of whether some of the recently discovered or controversial meson resonances, including glueball and hybrid candidates, can be accommodated as quarkonia.

*¹barnes@orph01.phy.ornl.gov ²fec@v2.rl.ac.uk ³prp@a13.ph.man.ac.uk ⁴swanson@unity.ncsu.edu

I. INTRODUCTION.

Theoretical studies of light hadron spectroscopy have led to the widespread belief that gluonic excitations are present in the spectrum of hadrons, so more resonances should be observed than are predicted by the conventional $q\bar{q}$ and qqq quark model. The two general categories of gluonic mesons expected are glueballs (dominated by pure glue basis states) and hybrids (dominated by basis states in which a $q\bar{q}$ is combined with a gluonic excitation).

Some of these novel states, notably the light hybrids, are predicted to have exotic quantum numbers (forbidden to $q\bar{q}$), such as $J^{PC} = 1^{-+}$. The confirmation of such a resonance would be proof of the existence of exotic non- $q\bar{q}$ states, and would be a crucial step towards establishing the spectrum of gluonic states. There are detailed theoretical predictions for the decays of these exotic hybrids [1,2], which have motivated several experimental studies of purportedly favored hybrid channels such as $b_1\pi$ and $f_1\pi$.

Although one would prefer to find these unambiguously non- $q\bar{q}$ J^{PC} -exotics, glueballs and hybrids with non-exotic quantum numbers are also expected. For example, in the flux tube model the lowest hybrid multiplet, expected at ≈ 1.8 -1.9 GeV [3,4], contains the non-exotics $J^{PC} = 0^{-+}, 1^{\pm\pm}, 1^{+-}$ and 2^{-+} in addition to the exotics $0^{+-}, 1^{-+}$ and 2^{+-} . To identify these non-exotic states one needs to distinguish them from the “background” of radial and orbital $q\bar{q}$ excitations in the mass region ≈ 1.5 -2.5 GeV, where the first few gluonic levels are anticipated [5,6].

Our point of departure is to calculate the two-body decay modes of all radial and orbital excitations of $n\bar{n}$ states ($n = u, d$) anticipated up to 2.1 GeV. This includes 2S, 3S, 2P, 1D and 1F multiplets, a total of 32 resonances in the $n\bar{n}$ sector. We also summarize the experimental status and important decays of candidate members of these multiplets, and compare the predictions for decay rates with experiment.

We start by briefly reviewing the established 1S and 1P states that confirm that 3P_0 pair creation dominates most hadronic decays. SHO wavefunctions are employed for

convenience; these lead to analytic results for decay amplitudes and are known to give reasonable empirical approximations. This is sufficient for our main purpose, which is to emphasize selection rules and to isolate major modes to aid in the identification of states. In addition to the 1S and 1P states we also find reasonable agreement between the model and decays of 1D, 2P and 1F states where data exist; this confirms the extended utility of the model and adds confidence to its applications to unknown states.

Examples of new results include the following.

- The radial 2^3P_1 $a_{1R} \rightarrow \rho\pi$ is strongly suppressed in S-wave, and dominant in D-wave. This contrasts with the expectation for a hybrid a_1 . The model's prediction of a dominant D-wave has been dramatically confirmed for the $a_1(1700)$ [7,8] and thereby establishes 1.7 GeV as the approximate mass of the $n\bar{n}$ members of the 2P nonets. This includes the 0^{++} nonet whose $I=0$ members share the quantum numbers of the scalar glueball.

- In the scalar glueball sector, we find that the decays of the $f_0(1500)$ and the $f_J(1710)$ are inconsistent with radially excited quarkonia.

- We identify the 2S 0^{-+} nonet. The η members are predicted to have narrow widths relative to the π counterpart. This is consistent with the broad $\pi(1300)$ and the narrower candidates $\eta(1295)$ and $\eta(1440)$.

- The vector states $\rho(1465)$ and $\omega(1419)$ are interesting in that the decay branching fractions appear to show anomalous features requiring a hybrid component. We identify the experimental signatures needed to settle this question.

- The $\pi(1800)$ has been cited as a likely hybrid candidate [2,9,10] on the strength of its decay fractions. The 3S 0^{-+} $q\bar{q} \pi$ is also anticipated in this region. We find that the decays of the hybrid and 3S 0^{-+} have characteristic differences which enable them to be distinguished. We identify modes that may enable the separation of these two configurations.

Our other results for the many $n\bar{n}$ states predicted up to 2.1 GeV should be useful in

the identification of these higher quarkonia, and in confirming that non-exotic gluonic or molecular states are indeed inconsistent with quarkonium assignments.

The order of discussion is 1S and 1P (section 2); 2S and 3D_1 (section 3); 3S (section 4); 2P (section 5); 1D (section 6); 1F (section 7). A summary and an outline for experimental strategy is in section 8.

II. 1S AND 1P TESTBED

First we will use the well known decays of light 1S and 1P $n\bar{n}$ states to motivate and constrain the 3P_0 decay model. Ackleh, Barnes and Swanson [11] have carried out a systematic study of $q\bar{q}$ decays in the 3P_0 and related pair creation decay models: in that work a 3P_0 -type amplitude was established as dominant in most light $n\bar{n}$ decays. (For other discussions of $q\bar{q}$ decays in the 3P_0 model see Ref. [13]). Fig.1, from Ref. [11], shows 3P_0 model predictions for the decay widths. Large widths are indeed predicted to be large and smaller widths are found to be correspondingly small. If we choose the pair creation strength $\gamma = 0.5$ (Eq. A3) to set an approximately correct overall width scale, then $\Gamma(h_1 \rightarrow \rho\pi)$ and $\Gamma(a_1 \rightarrow \rho\pi)$ are both ≈ 0.4 - 0.5 GeV; $\Gamma(f_2 \rightarrow \pi\pi)$, $\Gamma(\rho \rightarrow \pi\pi)$ and $\Gamma(b_1 \rightarrow \omega\pi)$ are all ≈ 0.1 - 0.2 GeV, and $\Gamma(a_2 \rightarrow \rho\pi)$ is smallest, ≈ 0.05 GeV; all are reasonably close to the observed widths.

The optimum parameter values found in a fit to the partial widths of Fig.1 [11] are $\beta = 0.40$ GeV (which is actually the length scale most commonly used in light $q\bar{q}$ decays) and $\gamma = 0.51$; with these values the rms relative error for these six decays is $\Delta\Gamma/\Gamma_{expt} = 29\%$. In this work we have actually found that the pair production amplitude $\gamma = 0.5$ is somewhat large for higher-L $q\bar{q}$ states, so in our discussions of higher quarkonia we will instead use $\gamma = 0.4$. In constrained- γ fits we find that using $\gamma = 0.4$ only moderately decreases the accuracy of the fit to the light 1S and 1P decays, to $\Delta\Gamma/\Gamma_{expt} = 43\%$, with an optimum $\beta = 0.36$ GeV.

A more sensitive test of the 3P_0 model involves amplitude ratios in the decays $b_1 \rightarrow \omega\pi$

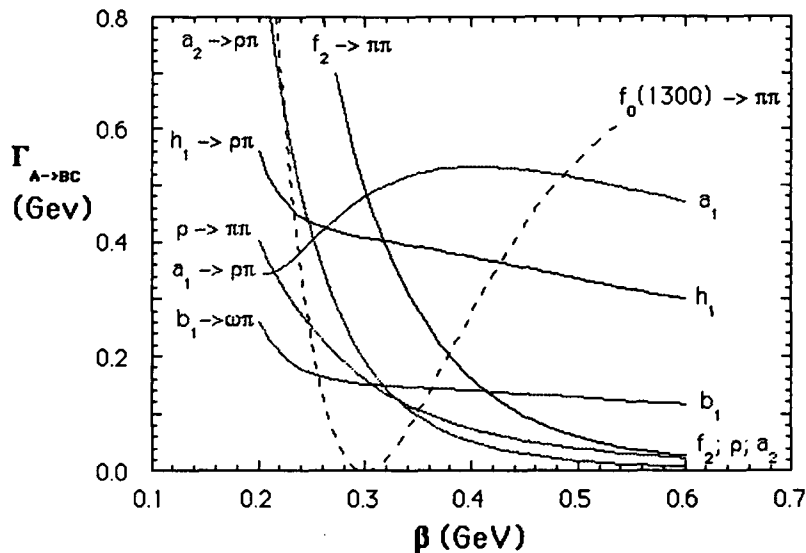


Figure 1. Partial widths of light 1S and 1P $q\bar{q}$ mesons in the 3P_0 model. The model parameters shown are $\beta = 0.2\text{--}0.6$ GeV (with $\beta \approx 0.4$ GeV preferred) and $\gamma = 0.5$.

and $a_1 \rightarrow \rho\pi$. In these decays both S- and D-wave final states are allowed, and the ratio of these decay amplitudes is known to be $D/S = +0.260(35)$ for the b_1 and $-0.09(2)$ for the a_1 [14]. This ratio is quite sensitive to the quantum numbers of the produced pair; with 3P_0 quantum numbers and the usual β we find reasonable agreement in sign and magnitude, whereas a OGE pair production mechanism gives the wrong sign for D/S [11]. This ratio test for $b_1 \rightarrow \omega\pi$ was historically very important in establishing the 3P_0 decay model [12].

These successes of the 3P_0 model motivate its use in predicting decays of the less familiar radial and orbital excitations of light quarkonia.

III. 2S STATES

We first consider the decays of the low-lying radially-excited pseudoscalar and vector states. Our general approach will be to review recent data on the state in question and

compare these data to predictions for candidate $q\bar{q}$ and (where appropriate) hybrid states. In each case we will attempt to identify decay modes that distinguish between competing assignments most clearly.

A. $0^{-+} 2^1S_0$: π and η

- $\pi(1300)$

The $\pi(1300)$ was first reported by Bellini *et al.* [15] in 1982 but remains rather poorly known. It is seen in $\pi\rho$, $\pi(\pi\pi)_S$ and $\pi f_0(1300)$, with a width of 200-600 MeV; there is however no accurate measurement of the branching fractions [16]. Recently higher statistics have been obtained for the $\pi(1300)$ by VES [7,10] and by E852 at BNL [8]. The VES data shows a clear $\pi(1300)$ peak in 3π , with a width of $\Gamma \approx 400$ -500 MeV in both $\pi(\pi\pi)_S$ and $\rho\pi$; the latter is particularly strong and dominates this channel below 2 GeV.

It should be noted, however, that the size of the Deck background in $\pi(\pi\pi)_S$ is uncertain, and it is not clear whether the $\pi(1300)$ reported in $\pi(\pi\pi)_S$ is actually due to the resonance. Fig.1c of Ref. [7] suggests that the Deck mechanism could cause *all* of the $\pi(1300) \rightarrow \pi(\pi\pi)_S$ enhancement in Fig.4a of that reference. We will assume that this is essentially correct, and that the $\pi(1300)$ resonance decays dominantly to $\rho\pi$.

In the 3P_0 decay model we expect $\rho\pi$ to be the dominant mode of a $2S$ $q\bar{q}$ $\pi(1300)$, since this is the only open two-body channel. (We assume that the $f_0(980)$ and $a_0(980)$ are dominantly $K\bar{K}$, so the mode $\pi(1300) \rightarrow f_0(980)\pi$ is a more complicated three body or virtual two-body decay.) With our parameter set $\gamma = 0.4$ and $\beta = 0.4$ GeV we predict a partial width of

$$\Gamma(\pi(1300) \rightarrow \pi\rho) = 209 \text{ MeV} . \quad (1)$$

This rate is given in Table B2 of Appendix B. (App.B is a tabulation of all our numerical results for partial widths in the 3P_0 model.) In Fig.2 we show the dependence of this prediction on the wavefunction length scale β . Evidently the prediction of a large width,

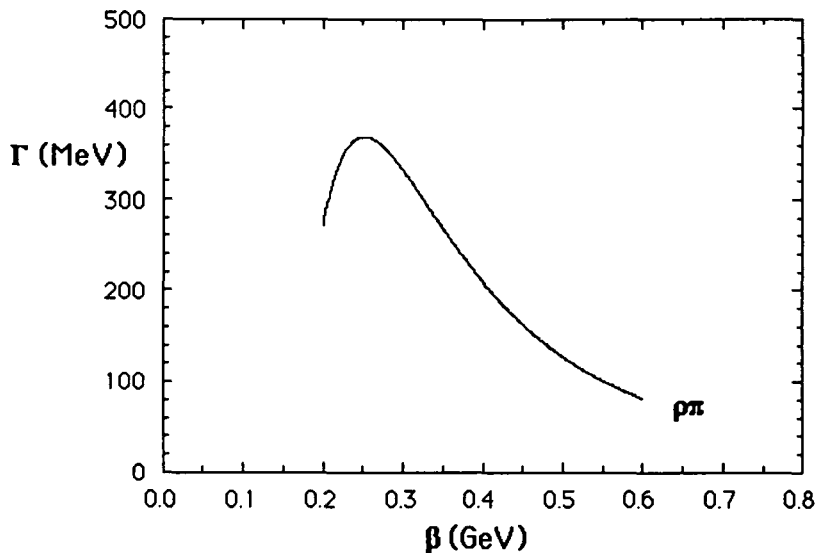


Figure 2. The $\rho\pi$ partial width of a $2S$ $\pi(1300)$, with 3P_0 model parameters $\beta = 0.2$ - 0.6 GeV and $\gamma = 0.4$.

comparable to observation, follows from any plausible choice for β . Thus the observed $\pi(1300)$ is consistent with expectations for a 2^1S_0 $q\bar{q}$ state.

Although the mode $f_0^{q\bar{q}}(1300)\pi$ is nominally closed by phase space, the $f_0(1300)$ is a very broad state, so one might anticipate a significant $(\pi\pi)_S\pi$ mode through the low-mass tail of the $f_0(1300)$. This possibility may be tested by varying $M(f_0^{q\bar{q}})$; the resulting $\Gamma(\pi(1300) \rightarrow f_0^{q\bar{q}}\pi)$ does not exceed 10 MeV over the range $M(f_0^{q\bar{q}}) = 400$ - 1000 MeV. Thus, the population of a $\pi(\pi\pi)_S$ mode by $\pi(1300)$ decays through an intermediate $f_0^{q\bar{q}}\pi$ state is predicted to be a small effect. If there actually is a large $\pi(1300) \rightarrow \pi(\pi\pi)_S$ mode, rather than a nonresonant Deck effect, this would be in disagreement with the 3P_0 model. Thus it would be very interesting to establish the branching fraction for $\pi(1300) \rightarrow \pi(\pi\pi)_S$ accurately in future work.

- $\eta(1295)$

This state has a width of $\Gamma = 53(6)$ MeV [16], much narrower than its $I=1$ 2^1S_0

partner $\pi(1300)$. It has been reported in $a_0(980)\pi$ and $\eta\pi\pi$. This small width is natural if the $\pi(1300)$ does indeed decay dominantly to $\rho\pi$, since G-parity forbids the analogous processes $\eta_{n\bar{n}} \rightarrow \rho\pi$ and $\eta_{n\bar{n}} \rightarrow \omega\eta$; to the extent that the $a_0(980)$ and $f_0(980)$ are dominantly $K\bar{K}$ there are no quasi-two-body $q\bar{q}$ modes open to the $\eta(1295)$. Consequently the decays must proceed through the weaker direct three-body and virtual two-body channels such as $a_0^{q\bar{q}}\pi$ and $f_0^{q\bar{q}}\eta$.

It is interesting to note the rôle that the 2S initial wavefunction has played in our discussion. Suppose for illustration that we had instead used 1S wavefunctions for the $\pi(1300)$ and $\eta(1295)$; we would then have predicted partial widths of several hundred MeV into the low-energy tails of the modes $f_0^{q\bar{q}}\pi$ and $a_0^{q\bar{q}}\pi$, with consequent broad widths for the $\pi(1300)$ and the $\eta(1295)$, in contradiction with experiment.

- $\eta(1440)$

These successes raise provocative questions regarding the $\eta(1440)$ state(s). This is a purportedly complicated region which may contain more than one resonance [16]. The PDG width of the $\eta(1440)$ is only $\Gamma = 60(30)$ MeV, with signals reported in K^*K , $a_0(980)\pi$, $\eta(\pi\pi)_S$ and $\rho\gamma$.

Except for $\rho\gamma$ these modes are not inconsistent with a dominantly $s\bar{s}$ state. The only two-body strong channel open for a 2^1S_0 $s\bar{s}$ $\eta(1440)$ is K^*K , but this could rescatter from $KK\pi$ into the other reported modes $a_0(980)\pi$ and $\eta\pi\pi$. The 3P_0 model prediction for the partial width $\eta(1440) \rightarrow K^*K$ versus the wavefunction length scale β is shown in Fig.3. Evidently the predicted K^*K partial width is comparable to the observed width, so a 2^1S_0 $s\bar{s}$ assignment appears possible for this state.

Of course the $\rho\gamma$ mode is not expected from $s\bar{s}$, and if confirmed may imply large $n\bar{n} \leftrightarrow s\bar{s}$ mixing in this sector as is observed in the 1S $I=0$ pseudoscalars. This can be parameterized as

$$|\eta(1295)\rangle = +\cos(\theta)|n\bar{n}\rangle + \sin(\theta)|s\bar{s}\rangle \quad (2)$$

$$|\eta(1440)\rangle = -\sin(\theta)|n\bar{n}\rangle + \cos(\theta)|s\bar{s}\rangle . \quad (3)$$

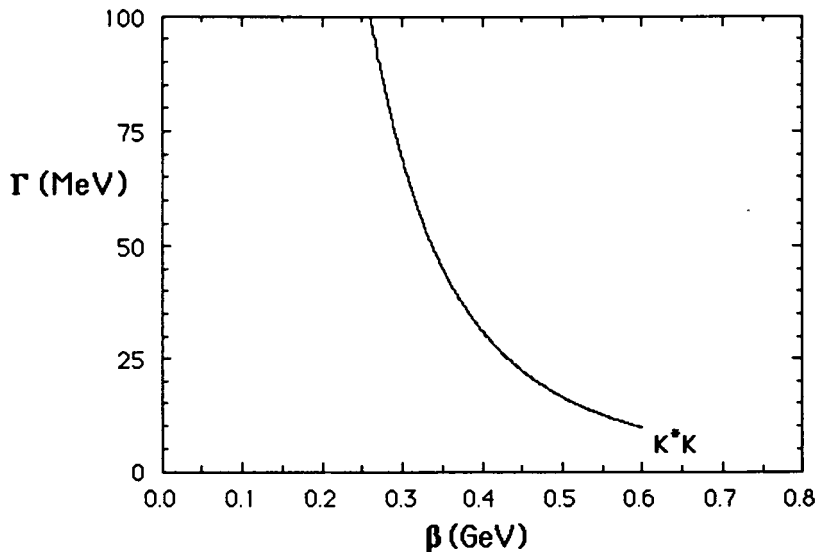


Figure 3. The $K^*\bar{K} + \text{h.c.}$ partial width of a 2^1S_0 $s\bar{s}$ $\eta(1440)$ in the 3P_0 model. Other two-body modes are excluded by phase space.

(4)

A remeasurement of $\eta(1440) \rightarrow \rho\gamma$, which should be possible at BEPC and TCF in $\psi \rightarrow \gamma\gamma\rho$, would be very useful in clarifying the nature of this state. Ideally we would like to know the invariant mass distributions of $\rho\gamma$, $\omega\gamma$ and $\phi\gamma$ final states, since these are flavor-tagging modes that allow investigation of possible flavor mixing in the parent resonances. Similarly, an accurate measurement of the branching fractions in the flavor-tagging $\psi \rightarrow V\eta(1440)$ and $V\eta(1295)$ hadronic decays, with $V = \omega, \phi$, would be useful for the determination of the $n\bar{n}$ - $s\bar{s}$ mixing angle.

In summary, from the total widths alone it is possible to describe the $\eta(1295)$ and $\eta(1440)$ as unmixed $n\bar{n}$ and $s\bar{s}$ 2^1S_0 radial excitations. The report of a large $\eta(1440) \rightarrow \rho\gamma$ radiative mode however suggests flavor mixing between these states, and should be remeasured with greater sensitivity together with other $V\gamma$ modes. This mixing could also account for the large $\eta(1440)$ signal seen in $\eta(\pi\pi)$ by GAMS [17].

B. 1^{--} : 2^3S_1 and 3D_1 ρ and ω

• $\rho(1465)$, $\rho(1700)$

If one accepts that the $\pi(1300)$ and $\eta(1295)$ belong to a 2^1S_0 $q\bar{q}$ nonet, it is then natural to assign the $\rho(1465)$ and the $\omega(1419)$ [16,18] to 2^3S_1 states. Indeed, one expects the contact hyperfine interaction to raise the mass of the vector nonet with respect to the pseudoscalar nonet by approximately this amount [19]. It is unlikely that the vectors near 1.4-1.5 GeV are dominantly D-waves, since the 3D_1 $n\bar{n}$ states should lie close to the other 1D candidates such as the $\pi_2(1670)$, $\rho_3(1691)$ and $\omega_3(1667)$. In the Godfrey-Isgur potential model a mass of 1660 MeV was predicted for the 3D_1 state, whereas they expect the 2^3S_1 radial excitation at 1450 MeV [19]. The $\rho(1465)$ also lies well below flux-tube model expectations of $M_H(1^{--}) \approx 1.8$ -1.9 GeV [3,4] for vector hybrids, so although the possibility of light vector hybrids has been discussed [2,20], these do not appear likely unless the flux tube model for hybrids is misleading.

The experimental branching fractions of these 1^{--} states are somewhat obscure, because there are at least two broad, overlapping resonances in each flavor sector in this mass region. The status of these vector states as seen in e^+e^- annihilation was reviewed recently by Clegg and Donnachie [18]. In the ρ sector they find that at least two states are present. The lighter state is assigned a mass of $M = 1.463(25)$ GeV and a width of $\Gamma = 0.311(62)$ GeV; it couples strongly to 4π states (including $a_1\pi$ but not $h_1\pi$) and $\omega\pi$, and less strongly to $\pi\pi$. The higher state has $M = 1.73(3)$ GeV, $\Gamma = 0.40(10)$ GeV, couples most strongly to 4π ($a_1\pi$ and $h_1\pi$ are not separated) and perhaps 6π ; $\pi\pi$ is also important, but the $\omega\pi$ width is found to be small.

These states have also been reported recently by Crystal Barrel [21] in $\pi^-\pi^0$ states in $\bar{p}d \rightarrow \pi^-\pi^0\pi^0p$; both vectors appear in $\pi^-\pi^0$, with masses and widths of $M = 1.411(10)(10)$ GeV, $\Gamma = 0.343(18)(8)$ GeV, and $M = 1.780^{+34}_{-25}(14)$ GeV, $\Gamma = 0.275(42)(17)$ GeV, quite similar to the e^+e^- results.

The 3P_0 model predictions for pure 2^3S_1 and 3D_1 ρ states at 1.465 GeV and 1.700 GeV

TABLE I. Partial widths of 2S, 1D and hybrid ρ states.

	$\pi\pi$	$\omega\pi$	$\rho\eta$	$\rho\rho$	KK	K^*K	$h_1\pi$	$a_1\pi$	total
$\rho_{2S}(1465)$	74.	122.	25.	-	35.	19.	1.	3.	279.
$\rho_{1D}(1700)$	48.	35.	16.	14.	36.	26.	124.	134.	435.
$\rho_H(1500)$	0	5	1	0	0	0	0	140	≈ 150

are given in Table I (see also Tables B1, B8), together with flux tube model predictions for a hypothetical 1.5 GeV vector hybrid. Very characteristic differences between the states are evident in their couplings to 4π final states; 2S couples very weakly to these, 1D couples strongly to both $a_1\pi$ and $h_1\pi$, and the hybrid couples strongly to $a_1\pi$ but not to $h_1\pi$. Both quarkonium states have moderately large couplings to $\pi\pi$ and $\omega\pi$, whereas the hybrid couples strongly only to $a_1\pi$.

Note that the $|q\bar{q}\rangle$ components are spin *triplet* whereas the hybrid is spin *singlet*. This difference in spin underlies the characteristic pattern of branching fractions in Tables I and II.

Although there are many similarities between theory and experiment, there are problems in detail. The important couplings of the lighter state to $\pi\pi$ and $\omega\pi$ found by Clegg and Donnachie are consistent with a 2S quarkonium, but we do not expect a significant coupling of a 2^3S_1 ρ to 4π final states. The dominant coupling of the heavier state to 4π is as predicted for the D-wave quarkonium, but the reported absence of $\omega\pi$ is not expected. The presence of two states (2^3S_1 and $3D_1$) in $\pi\pi$ with comparable strengths, reported by Crystal Barrel [21], is expected.

Of course it is difficult to distinguish the contributions from two broad states with similar masses, and the 4π final states themselves have not yet been completely characterized. (The $a_1\pi$ and $h_1\pi$ modes of the $\rho(1700)$ in e^+e^- for example have not been separated.) It appears likely that the states and their branching fractions are still inadequately resolved experimentally in this mass region, so it is not yet appropriate to attempt a detailed fit,

TABLE II. Partial widths of 2S, 1D and hybrid ω states.

	$\rho\pi$	$\omega\eta$	KK	K^*K	$b_1\pi$	total
$\omega_{2S}(1419)$	328.	12.	31.	5.	1.	378.
$\omega_{1D}(1649)$	101.	13.	35.	21.	371.	542.
$\omega_H(1500)$	20	1	0	0	0	≈ 20

using for example linear combinations of the 2S and 1D basis states.

It is clear from our 3P_0 results that in future it will be important to separate the $a_1\pi$ and $h_1\pi$ contributions (which tag 1D and H [2,20] states), and that the $\pi\pi$ and $\omega\pi$ distributions should also be studied carefully, since these are expected to arise mainly from quarkonia rather than hybrids.

• $\omega(1419)$ and $\omega(1649)$

We anticipate similar problems with at least two broad overlapping resonances in the $I=0$ sector. Clegg and Donnachie [18] discuss both one- and two-resonance fits to the ω sector in the reactions $e^+e^- \rightarrow \rho\pi$ and $\omega\pi\pi$. In their two-resonance fit they find a lower state with a mass and width of $M = 1.44(7)$ GeV, $\Gamma = 0.24(7)$ GeV, and a higher, quite narrow state with $M = 1.606(9)$ GeV, $\Gamma = 0.113(20)$ GeV. The PDG quote masses and widths of $M = 1.419(31)$ GeV, $\Gamma = 0.174(59)$ GeV, $M = 1.649(24)$ GeV, $\Gamma = 0.220(35)$ GeV; the parameters for the lighter state are consistent but the width of the higher-mass ω state is broader than Clegg and Donnachie estimate.

Clegg and Donnachie find that both ω states couple strongly to $\rho\pi$. Only the second is found to couple to $\omega\pi\pi$, and that coupling is rather weak. A fit with a single resonance finds instead that the $\omega\pi\pi$ branching fraction exceeds $\rho\pi$, so these should be regarded as tentative conclusions.

For comparison we again show the numerical predictions of the 3P_0 model for pure 2S, 1D and H states. The masses assumed are 1996 PDG values (see Tables B1 and B9). The large $\rho\pi$ couplings reported for the vector states are evidently consistent with

expectations for both 2S and 1D quarkonia. Again the S+S modes are predicted to be small for a hybrid, so they can be used to tag quarkonia or the $q\bar{q}$ components of mixed states. Since none of the favored S+P modes is open to an I=0 hybrid at 1.5 GeV, such a state would be quite narrow, as shown in Table II. (The decay $\omega_H \rightarrow b_1\pi$ is excluded by the “singlet selection rule” [2,11], which states that $(S_{q\bar{q}} = 0) \not\rightarrow (S_{q\bar{q}} = 0) + (S_{q\bar{q}} = 0)$ in the 3P_0 model; the ω_H hybrid has $S_{q\bar{q}} = 0$ in the flux tube model. Interestingly, the singlet selection rule holds for both 3P_0 and OGE quarkonium decay amplitudes [11].)

A hybrid in this mass region should be visible as a narrow bump in the $\rho\pi$ invariant mass distribution. (This channel is not favored for a hybrid, but it is allowed at a reduced rate due to different ρ and π spatial wavefunctions.) Thus it may be useful to search $\rho\pi$ final states for narrow resonances with improved statistics, although the signal would of course be broadened by the ρ width.

The very large $b_1\pi$ mode predicted for the 1D quarkonium is very interesting, because neither 2S nor hybrid vector states are expected to couple significantly to $b_1\pi$. This two-body mode will appear as $\omega\pi\pi$; Clegg and Donnachie do report an $\omega\pi\pi$ mode for their higher ω state, but the coupling is not as strong as we predict. The total width of their higher-mass state is also much smaller than expected. Since the 1D state is predicted to have a very large width, ≈ 500 MeV (Table B9), this discrepancy may be due to a distortion of the shape by threshold effects, with resulting inaccuracies in the reported couplings. Assuming that the 3P_0 model predictions are approximately correct, a study of the $1^{--} \omega\pi\pi$ mass distribution should reveal the $^3D_1 \omega$ basis state in isolation. (It may be distributed over several resonances.) If the quasi-two-body approximation is correct, the mass distribution of $\omega\pi$ pairs in the resonance contribution to $\omega\pi\pi$ should be consistent with a $b_1(1231)$.

C. Mixing in the 1^{--} sector.

Although we have considered the decay modes of pure 2S, 1D and H vector states, the physical resonances are certainly linear combinations of these and other basis states. Since the known resonances have similar masses, we should consider the possibility that there is significant mixing and introduce the linear combination

$$|V\rangle = \cos(\theta) \left(\cos(\phi) |2^3S_1\rangle + \sin(\phi) |^3D_1\rangle \right) + \sin(\theta) |H\rangle . \quad (5)$$

The mixing angles for each resonance can be determined from the branching fractions to certain states. The S+S modes identify the $q\bar{q}$ components of the state (see Tables I and II). In the $I=1$ states the 4π modes $a_1\pi$ and $h_1\pi$ are similarly characteristic; the $h_1\pi$ mode is produced only by the 1D basis state, and $a_1\pi$ comes from both 1D and hybrid states. Similarly in $I=0$ the mode $b_1\pi$ tags the 1D quarkonium basis state and 2S and 1D states both lead to strong $\rho\pi$ couplings. Determination of the mixing angles in the physical states will be possible given accurate measurements of the branching fractions to these characteristic modes.

We have not carried out a fit to determine the mixing angles because the experimental results do not yet appear definitive. However we note that the partial widths reported by Clegg and Donnachie for the $\rho(1465)$, which include a large $\Gamma_{a_1\pi}$ and a small $\Gamma_{h_1\pi}$, are inconsistent with 2S or 1D alone. These widths imply a large H component in this state with the possibility of considerable H-2S mixing.

Future experimental work could concentrate on an accurate determination of the $\pi\pi$, $\omega\pi$, $h_1\pi$ and $a_1\pi$ branching fractions of the ρ states. The $h_1\pi$ and $a_1\pi$ modes are especially sensitive to the nature of the initial state. Similarly the $\rho\pi$ and $b_1\pi$ branching fractions of the ω states are the most interesting experimentally.

TABLE III. Partial widths of 3S and hybrid $\pi(1800)$ states.

	$\rho\pi$	$\rho\omega$	$\rho(1465)\pi$	$f_0(1300)\pi$	$f_2\pi$	K^*K	total
$\pi_{3S}(1800)$	30.	74.	56.	6.	29.	36.	231.
$\pi_H(1800)$	30	0	30	170	6	5	≈ 240

IV. 3S STATES

A. $0^{-+} : 3^1S_0 \pi(1800)$

The same experiments [7,10,15,22] that see the $\pi(1300)$ in $\rho\pi$ and a possible broad enhancement in $\pi(\pi\pi)_S$ also report a prominent $\pi(1800)$ in $f_0(980)\pi$, $f_0(1300)\pi$, $f_0(1500)\pi$ and $K(K\pi)_S$. None of these experiments see the $\pi(1800)$ in $\rho\pi$. This is striking, as also is the fact that the total width of ≈ 150 -200 MeV is considerably smaller than that of the $\pi(1300)$. Furthermore, the presence of clear signals in both $f_0(1300)\pi$ and $f_0(980)\pi$ is remarkable and was commented upon with some surprise [10].

The decays into $\pi\rho$ and KK^* are both suppressed; VES quote the limits [10]

$$\frac{\pi(1800) \rightarrow \pi^- \rho^0}{\pi(1800) \rightarrow \pi^- f_0(980)|_{\rightarrow \pi^+ \pi^-}} < 0.14 \quad (90\% \text{ c.l.}) \quad (6)$$

and

$$\frac{\pi(1800) \rightarrow K^- K^*}{\pi(1800) \rightarrow K^- K^+ \pi(S - wave)} < 0.1 \quad (95\% \text{ c.l.}) . \quad (7)$$

A prominent KK_0^* signal is present (observed as $K(K\pi)_S$), so the virtual transition $\pi(1800) \rightarrow KK_0^* \rightarrow KK\pi \rightarrow f_0(980)\pi$ is probably responsible for the coupling to $f_0(980)\pi$; this mode appears to be stronger than $f_0(1300)\pi$. The mass of this state makes it a candidate for either the radial 3^1S_0 or the ground state hybrid π_H . The predicted branching fractions for 3^1S_0 (Table B4) and π_H hybrid states (from Ref. [2]) near this mass are shown in Table III.

The decay amplitude for $3^1S_0 \rightarrow 3^1S_1 + 1^1S_0$ is actually close to a node with these masses, so the weak coupling to $\rho\pi$ is expected for both a 3S quarkonium and a hybrid. The most

important differences are in the $\rho\omega$ and $f_0(1300)\pi$ modes: $\rho\omega$ is predicted to be the largest mode of a 3S $\pi(1800)$ state, whereas for a hybrid $\pi_H(1800) \rightarrow \rho\omega$ should be very weak (this is the usual selection rule against S+S final states). Conversely, $f_0(1300)\pi$ is predicted to be weak for 3S quarkonium but is expected to be the dominant decay mode of a $\pi_H(1800)$ hybrid. The observation of a large $f_0(1300)\pi$ mode argues in favor of a hybrid assignment for this state. One should note however that the 3P_0 model also predicts a small branching fraction for $\pi(1300) \rightarrow \pi(\pi\pi)_S$; if the observed $\pi(\pi\pi)_S$ signal is really due to the $\pi(1300)$ rather than the Deck effect, the decay model may simply be inaccurate for $N^1S_0 \rightarrow ^1S_0 + ^3P_0$ transitions. There may for example be large OGE decay amplitudes in these channels, as was found in the related transition $^3P_0 \rightarrow ^1S_0 + ^1S_0$ [11]; this can be checked in a straightforward calculation [23]. Thus the presence of a strong $\pi(1800) \rightarrow f_0(1300)\pi$ mode is indicative of a hybrid *assuming* that the 3P_0 model is accurate.

Although the strong $f_0(1300)\pi$ signal in the VES data may well have isolated the $\pi_H(1800)$ hybrid, VES also finds evidence for a large $\rho\omega$ signal at a similar mass [24]. We expect $\rho\omega$ to arise from the 3S $\pi(1800)$ quarkonium state rather than from a hybrid. These signals may be due to two different resonances; the $\rho\omega$ signal is evident well below 1800 MeV, and persists to higher mass than the $f_0(1300)\pi$ distribution. Similarly the mode $f_2\pi$ is observed (Fig.4d of Ref. [7]), but at a mass of ≈ 1700 MeV, well below the $\pi(1800)$ seen in $f_0(1300)\pi$. This may also indicate a 3S state somewhat below a hybrid $\pi(1800)$. If two 0^{-+} π resonances were to be isolated in this region, this would be strong evidence through overpopulation for both a hybrid and a 3S $q\bar{q}$ excitation.

Further investigation of the modes $\rho\pi$, $\rho(1465)\pi$, $\rho\omega$, $f_0(1300)\pi$ and $f_2\pi$ could be useful to clarify the resonances in the region of the $\pi(1800)$; establishing the branching fractions to these states is especially important. The most characteristic are $\rho\omega$ and $f_0(1300)\pi$, since the hybrid and 3S quarkonium predictions differ greatly for these modes. Theoretical studies of the stability of the decay amplitudes under variation of parameters

and wavefunctions and the assumed decay mechanism [11] would also be interesting.

Searches for the multiplet partners of this state may be useful, since they too have characteristic decay modes. A 3S $n\bar{n}$ $\eta(1800)$ quarkonium for example (Table B4) is predicted to have large $\rho\rho$ and $\omega\omega$ modes, which should be zero for a hybrid. An $\eta(1760)$ which couples to $\rho\rho$ and $\omega\omega$ was reported by MarkIII [25] and by DM2 [26]. The conclusions regarding the presence of this pseudoscalar signal in the MarkIII 4π data have since been disputed [27].

B. $1^{--} : 3^3S_1$

If the $\pi(1800)$ is a 3S quarkonium we should expect to find 3S vector states near 1.9 GeV. No candidates for these states are known at present below 2.1 GeV, however there are possible ρ candidates at 2150 and 2210 MeV [16]. The predictions for decays of 3S vectors are given in Table B3; it is notable that the simple S+S modes have small couplings, with the exception of $\rho(1900) \rightarrow \rho\rho$. Unfortunately the relatively obscure 2S+S modes are favored, especially for the $\omega(1900)$. Some S+P modes have sufficiently strong couplings to the 3S vectors to be attractive experimentally, notably $\rho(1900) \rightarrow a_2\pi$ and $\omega(1900) \rightarrow b_1\pi$. As noted previously, the $b_1\pi$ mode is forbidden to an ω vector hybrid by the singlet selection rule, since this hybrid decay would have $S_{q\bar{q}} = 0$ for all states.

V. 2P STATES

The 2P states are especially important because the expected mass of this multiplet (≈ 1700 MeV) is close to the predicted mass of the lowest hybrid multiplet in the flux tube model, ≈ 1.8 -1.9 GeV [3,4]. Furthermore, the position of the 1P and 2P unmixed $n\bar{n}$ levels and the 1P $s\bar{s}$ level are needed for input to quarkonium - glueball mixing studies [28] based on the lattice expectations for glueballs in this region [5]. Determining the nature of the $f_J(1710)$ will be important in this regard. Since the quantum numbers 1^{++}

TABLE IV. Partial widths of 2P and hybrid $a_1(1700)$ states.

	$\rho\pi$	$\rho\omega$	$\rho(1465)\pi$	$b_1\pi$	$f_0(1300)\pi$	$f_1\pi$	$f_2\pi$	K^*K	total
$a_{1(2P)}(1700)$	57.	15.	41.	41.	2.	18.	39.	33.	246.
$a_{1(H)}(1700)$	30	0	110	0	6	60	70	20	≈ 300

and 1^{+-} occur in both the hybrid and 2P multiplets, these states need to be identified to avoid confusion with hybrids. As we shall see, a recently discovered 1^{++} state, the $a_1(1700)$, appears to be our first confirmed member of the 2P multiplet, in that it passes a very nontrivial 3P_0 model amplitude test and thereby for the first time establishes the mass scale of the 2P multiplets.

A. $1^{++} : 2^3P_1 a_1(1700)$

A recent experiment at BNL [29] reported a candidate 1^{-+} exotic, produced by $\pi\rho$ and decaying to πf_1 . They also see a 1^{++} state in this channel at ≈ 1.7 GeV, with a width of ≈ 0.4 GeV; the relative phase of the 1^{++} and 1^{-+} waves was used to support the claim of a resonant 1^{-+} . A similar 1^{++} signal has been reported by VES in $\rho\pi$ [7,10].

The challenge is to establish whether this 1^{++} $a_1(1700)$ is a hybrid $a_{1(H)}$ (perhaps a partner of the reported 1^{-+} exotic) or a radial 2^3P_1 $n\bar{n}$ state. The predicted total width of a 1^{++} $a_1(1700)$ hybrid in the model of Close and Page [2] is ≈ 300 MeV, comparable to the observed width. However the total width predicted for a $a_1(1700)$ 2^3P_1 $n\bar{n}$ state is similar, about 250 MeV (see Table B5). Some differences between these assignments are evident when we compare partial widths (see Table IV). Clearly the 2P state couples more strongly to S+S modes than does the hybrid, as usual, so an accurate determination of the branching fractions to $\rho\pi$ and $\rho\omega$ would be interesting. The other modes are less characteristic with the exception of $b_1\pi$, which should come exclusively from the quarkonium state. The absence of the decay $a_{1(H)} \rightarrow b_1\pi$ is a special case of the singlet selection rule cited previously as forbidding the transition $\omega_H \rightarrow b_1\pi$. We therefore

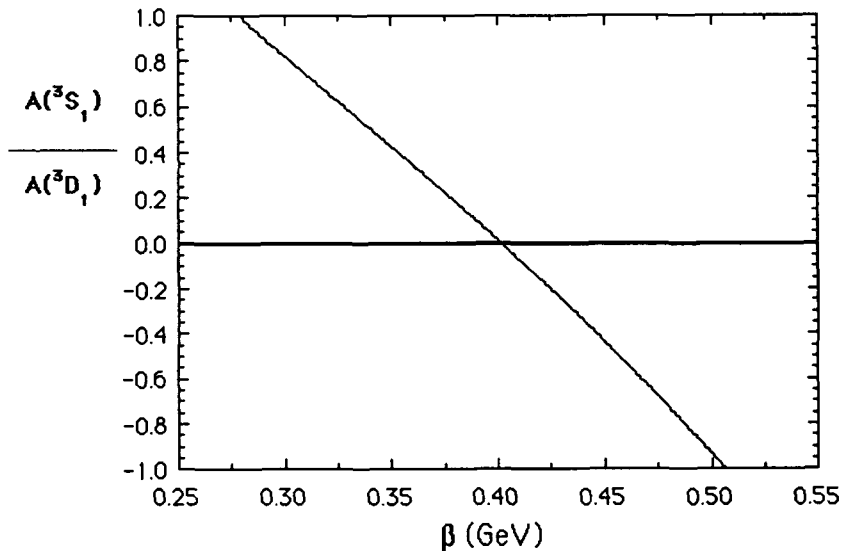


Figure 4. The S/D amplitude ratio in the transition $2^3P_1 \ a_1(1700) \rightarrow \rho\pi$ predicted by the 3P_0 model.

urge that experiments that observe $a_1(1700) \rightarrow \pi f_1$ also seek a signal, or a limit, for $a_1(1700) \rightarrow \pi b_1$.

A crucial test of 2P versus H assignments for the $a_1(1700)$ arises in the decay amplitudes to $\rho\pi$. From Appendix A, Eqs.(A53,A58,A59), the transition $2^3P_1 \rightarrow ^3S_1 + ^1S_0$ has both S and D amplitudes, and the D/S ratio is (where $x \equiv |\vec{p}_f|/\beta$)

$$\left. \frac{D}{S} \right|_{2^3P_1 \rightarrow ^3S_1 + ^1S_0} = -\frac{2^{1/27}}{3^{25}} \frac{x^2(1 - \frac{2}{21}x^2)}{(1 - \frac{4}{9}x^2 + \frac{4}{135}x^4)}. \quad (8)$$

The inverse of this ratio is shown versus β in Fig.4; note that the S-wave amplitude has a zero very close to the preferred value $\beta = 0.4$ GeV. This is a striking and unusual result, since in most cases we find that the lower partial waves are dominant. In contrast, for a hybrid one expects S-wave dominance, $a_{1(H)} \rightarrow (\rho\pi)_S : (\rho\pi)_D \approx 20 : 1$.

Experimentally, VES sees the $a_1(1700)$ prominently in the $\rho\pi$ D-wave (see Fig.2c of Ref. [7]); the resonance near 1.7 GeV dominates the entire 1-2 GeV region. In contrast, the $\rho\pi$ S-wave (Fig.2a of [7]) is dominated by the $a_1(1230)$ and shows no clear evidence

for the $a_1(1700)$. E852 similarly sees this resonance clearly in the $\rho\pi$ D-wave, with a mass and width of $M \approx 1.66$ GeV and $\Gamma \approx 0.22$ GeV [8]. This D-wave dominance of the $\rho\pi$ final state appears to be dramatic confirmation that the $a_1(1700)$ is a 2^3P_1 radial excitation. Furthermore the successful predictions of $a_1 \rightarrow \rho\pi$ being in S wave and $a_{1R} \rightarrow \rho\pi$ being in D wave supports the extension of the model to radial excitations.

With the $a_1(1700)$ established as a $2P$ $n\bar{n}$ state, the multiplet partners are expected nearby in mass (multiplet splittings due to spin-orbit and tensor forces appear to be small even at $L_{q\bar{q}} = 1$) and searches for these states should be carried out. In the next sections we will discuss the decay modes predicted for these other $2P$ states.

B. $0^{++}, 2^{++} \ 2^3P_0, 2^3P_2 : a_0(1700), a_2(1700)$

With the $a_1(1700)$ as the 2^3P_1 “ a_{1R} ” radial state, one may ask why the a_{0R} and a_{2R} partners are not seen in the same experiments. A simple explanation follows from the partial widths shown in Table B5. Since the production mechanism of the $a_1(1700)$ in $\pi p \rightarrow \pi f_1 p$ apparently involves natural parity exchange (probably ρ or f_2 exchange), the 0^{++} scalar state a_{0R} cannot be produced. Although the 2^{++} a_{2R} can be produced (note the large $\rho\pi$ coupling), it has a weak coupling to the πf_1 final state and hence is not readily observable in this channel.

There is some very recent evidence for a 2^3P_2 state from the Crystal Barrel, who report an $a_2(1650)$ in $\eta\pi^0$ final states in $p\bar{p} \rightarrow \eta\eta\pi^0$ [30]. Although we expect $\eta\pi$ to be a relatively minor mode, with a branching fraction of 7%, the mass and reported width of $\Gamma = 260(15)$ MeV are consistent with expectations (Table B5). The final states $\rho\pi$ and $\rho\omega$ are predicted to have large couplings to an a_{2R} state, so we expect a large signal in these 3π and 5π final states.

The prediction of a large coupling to vector meson pairs suggests $\gamma\gamma \rightarrow 2^3P_J \rightarrow VV$ as a possible source of the a_{0R} and a_{2R} states. Indeed, ARGUS has evidence that the $\rho\omega$ final state near threshold is mainly in the partial wave $J^{PC} = 2^{++}$, $J_z = 2$, and the $\gamma\gamma \rightarrow \rho^0\omega$

cross section is at maximum near 1.7 GeV [31]. The $J_z = 2$ signal is characteristic of a 2^{++} resonance, as there is a selection rule [32] that $\gamma\gamma \rightarrow (J = 2^{++}, \lambda = 0) = 0$ in the nonrelativistic quark model; hence $\lambda = 2$ dominates. A study of $\gamma\gamma \rightarrow 5\pi$ with improved statistics, perhaps at LEP2, may help to isolate these states. Of course the interpretation of any $\gamma\gamma \rightarrow VV$ reaction should be regarded as tentative until the large $\gamma\gamma \rightarrow \rho^0 \rho^0$ signal [33] is understood, as this reaction also is dominated by $J^{PC} = 2^{++}$, $J_z = 2$, but contains both $I=0$ and $I=2$ projections in s-channel and hence cannot come from a single $q\bar{q}$ resonance. Finally, the reaction $\gamma\gamma \rightarrow a_{0R} \rightarrow \pi b_1$ may also lead to a significant signal in 5π final states, and could be isolated if the $\lambda = 0$ selection rule is used to suppress the a_{2R} signal.

C. $2^{++} \ 2^3P_2 : f_2(1600 - 1800)$

Encouraged by the likely confirmation of the radial $1^{++} \ a_1(1700)$, we now turn our attention to the 2P isoscalar multiplet. First we consider the $f_2(1700) \ 2^3P_2 \ n\bar{n}$ radial tensor. We predict a large $\rho\rho$ width for the $2^3P_2 \ f_2(1700)$, and the modes $\omega\omega$, $\pi\pi$ and perhaps πa_2 should also be important (see Table B6). (Note that the simple branching fraction ratio $\rho\rho/\omega\omega \approx 3$ follows trivially from flavor counting.) The total width is predicted to be ≈ 400 MeV.

Although there is no strong evidence for such a state, there are suggestions of its presence in several processes. A large 2^{++} enhancement referred to as the $X(1600)$, with $\Gamma = 400(200)$ MeV, is well known in $\gamma\gamma \rightarrow \rho^0 \rho^0$ [14,34]. The small charged to neutral $\rho\rho$ ratio however precludes the identification of this signal with a single $f_2(1700)$ resonance. There are also reports of a rather narrow $f_2(1640)$ with a width of ≈ 60 -120 MeV in $\omega\omega$ [14,35-37]. Although the predicted $2^3P_2 \ f_2(1700)$ width is much larger, it would be reduced somewhat by threshold effects in the $\omega\omega$ channel. Indeed, if the resonance mass is around 1700 MeV and its width is several hundred MeV, as suggested by our analysis, it may decay strongly into $\rho\rho$ (due to the large ρ width leading to a favorable phase space),

but the narrowness of the ω may cause only the upper part of the resonance to feed the $\omega\omega$ channel. Thus the resonance width in $\omega\omega$ may appear smaller than in $\rho\rho$, so both the $X(1600)$ and the $f_2(1640)$ may be aspects of a single state.

A recent reanalysis of MarkIII data on $\psi \rightarrow \gamma\pi^+\pi^+\pi^-\pi^-$ [27] similarly sees evidence of a 2^{++} state near $M = 1.64$ GeV, with $\Gamma = 0.14$ GeV, which couples strongly to $\rho\rho$. (In contrast they observe 0^{++} states dominantly in $\sigma\sigma$.) This preference of the tensor state for $\rho\rho$ is consistent with 3P_0 model expectations for a 2^3P_2 $f_2(1700)$ state (Table B6).

Finally, it is possible that the $f_2(1520)$ or “AX” state seen in $p\bar{p} \rightarrow 3\pi$ [38] may be the low-mass tail of the $f_2(1700)$.

D. 0^{++} 2^3P_0 : $f_0(1500), f_J(1710)$

The 0^{++} f_0 sector in the 1.5 GeV mass region is clearly of interest for glueball searches. It is thus important to identify the 3P_0 quarkonia in this mass region. We stress that one should not be overly naive in this endeavor since strong recoupling effects, including couplings of quarkonia to nearby glueballs, are expected [28]. Nonetheless for initial theoretical guidance it will be useful to consider the predictions of the naive 3P_0 model for the decays of unmixed 3P_0 $n\bar{n}$ quarkonia.

The decays predicted for the 2P scalar $f_0(1700)$ state in the 3P_0 model are given in Table B6. Fortunately they are very characteristic. The dominant modes are $\rho\pi\pi$, with approximately equal contributions from $\pi(1300)\pi$ and $a_1(1230)\pi$. The channels $\rho\rho$ and $\pi\pi$ are also important, and the total width is predicted to be ≈ 400 MeV. The $\eta\eta$ and KK amplitudes are both close to nodes and are predicted to be quite small.

The two well known scalar resonances in this mass region which can be compared to these predictions are the glueball candidate $f_0(1500)$ and the $f_J(1710)$. These states have PDG masses and total widths of $M = 1503(11)$ MeV, $\Gamma = 120(19)$ MeV and $M = 1697(4)$ MeV, $\Gamma = 175(9)$ MeV; both are rather narrow relative to expectations for a 2P $n\bar{n}$ state. BES has recently reported [39] a spin parity analysis of the K^+K^- system in ψ radiative

decays; they see both $J=0$ and $J=2$ states. Both have widths of ≈ 100 MeV, much narrower than we expect for $2P$ $n\bar{n}$ states. The presence of a significant $\eta\eta$ mode for both the $f_0(1500)$ and $f_J(1710)$ argues against a $2P$ $n\bar{n}$ assignment. The possibility that a node in the $2P$ decay amplitude is consistent with the observed weakness of $f_J(1710) \rightarrow \pi\pi$ is found to be unrealistic in practice; although there are actually two nodes, the modes that are strongly suppressed by these in the 3P_0 model are $\eta\eta$ and KK , not $\pi\pi$.

The disagreement of predicted decay modes of $2P$ $n\bar{n}$ states with experiment for the $f_0(1500)$ and $f_J(1710)$ supports the suggestions that neither of these states is a quarkonium. Amsler and Close [28] have noted that the $f_0(1500)$ could be a glueball that is mixed with the nearby $n\bar{n}$ and $s\bar{s}$ basis states, which explains the observed branching fractions. Conversely, Weingarten [6] suggests that the $f_J(1710)$ is the scalar glueball, based on its mass and on lattice QCD evidence that flavor symmetry may be inaccurate in glueball decays, together with a different pattern of $q\bar{q} \leftrightarrow G$ mixing. It may be that the glueball, $n\bar{n}$ and $s\bar{s}$ basis states are all strongly mixed in this sector, so that an assumed separation into glueball and quarkonium states is inaccurate [40].

An alternative suggestion is that the $f_J(1710)$ may be a vector-vector molecule, analogous to the $f_0(980)$ and $a_0(980)$ $K\bar{K}$ candidates. The two possibilities discussed in the literature are $K^*\bar{K}^*$ [41] and $K^*\bar{K}^* + \omega\phi$ [42]; these both predict small nonstrange modes and large couplings to $KK\pi\pi$ final states. The weakness of the $\pi\pi$ mode is due to the presence of a hidden $s\bar{s}$ pair (just as for $f_0(980) \rightarrow \pi\pi$), since both models assume that the $f_J(1710)$ is dominantly $ns\bar{n}\bar{s}$ in flavor.

In any case the $2P$ scalar $n\bar{n}$ states (or resonances with large 2^3P_0 $n\bar{n}$ components) should appear in $\rho\pi\pi$ final states, so it would be useful to search for these states, especially in reactions that produce the $f_0(1500)$ or $f_J(1710)$.

Finally, we should consider the possibility that the $f_J(1710)$ is dominantly a 2^3P_2 $n\bar{n}$ tensor state (see Table B6), since the quantum numbers have not been determined definitively. Again the quarkonium assignment is inconsistent with experiment; the $\eta\eta$

coupling is predicted to be small, and $\pi\pi$ is predicted to be quite large. The largest mode, $\rho\rho$, has not been reported for the $f_J(1710)$. The total width of the $n\bar{n}$ state is again rather larger than reported for the $f_J(1710)$. One must conclude that the $f_J(1710)$ does not appear to be consistent with any $n\bar{n}$ quarkonium assignment.

E. $1^{+-} 2^1P_1$: $b_1(1700), h_1(1700)$

Predictions for the missing spin-singlet 2P states are given in Table B7. These are expected to be only about 250 MeV wide, so they may be easy to detect. Reactions that produce the $h_1(1170)$ and $b_1(1231)$ are obviously the most promising for searches for their radial excitations. The $h_1(1700)$ couples dominantly to $\rho\pi$, so it may be observable for example in $\pi^-p \rightarrow \rho\pi n$, in production through natural-parity exchange. Its partner $b_1(1700)$ can be produced similarly in $\omega\pi$ final states, and less characteristically in $\rho\rho$.

VI. 1D STATES:

A. $2^{-+} 1D_2$

Studies of the decays of hybrids in the flux tube model conclude that a 2^{-+} member of the lowest hybrid multiplet may be observably narrow [2]. This hybrid multiplet is expected at ≈ 1.8 -1.9 GeV [3,4], which overlaps the Godfrey-Isgur quark model predictions of 1.68 GeV for the $1D_2 n\bar{n}$, 1.89 GeV for $1D_2 s\bar{s}$, and 2.13 GeV for $2^1D_2 n\bar{n}$ [19]. Thus it may be necessary to use characteristic branching fractions to distinguish quarkonia from hybrids in this mass region. Of course the $\pi_2(1670)$ is presumably $n\bar{n}$ because it has well established 1D multiplet partners such as the $\rho_3(1691)$, but distinguishing the higher-mass $s\bar{s}$ and 2D quarkonia from hybrids may not be so straightforward.

B. π_2

Experimentally, the $\pi_2(1670)$ couples most strongly to $f_2(1275)\pi$ ($\approx 56\%$) and $\rho\pi$ ($\approx 31\%$), with weaker couplings (at the 5-10% level) to $f_0(1300)\pi$ and K^*K . The 1996 PDG total width is 258(18) MeV [14]. In comparison, the 3P_0 model predicts a total width of 250 MeV, with branching fractions of $f_2(1275)\pi$ ($\approx 30\%$), $\rho\pi$ ($\approx 47\%$) and K^*K ($\approx 12\%$); these are in reasonable qualitative agreement with experiment. There is however disagreement with experiment in that little $f_0(1300)\pi$ is expected; we predict a branching fraction of only 0.2% to this mode, whereas the PDG value is 8.7(3.4)%. The largest as yet unreported mode should be $\rho\omega$, predicted to have a branching fraction of 11%.

In addition to the plausible quarkonium state $\pi_2(1670)$, the ACCMOR Collaboration in 1981 noted a 2^{-+} structure near 1.8 GeV, coupled to $f_2\pi$ and weakly to $f_0(1300)\pi$ and $\rho\pi$ [43]. This is similar to reports of a possible 2^{-+} (or even 1^{-+}) seen in photoproduction of 3π states near 1.77 GeV with a width of 100-200 MeV, which couples to $\rho\pi$ and $f_2\pi$ [44]. The VES Collaboration also claims a peak near 1.8 GeV, which they believe however to be non-resonant [45]. Lastly, two-photon experiments which see the $\pi_2(1670)$ in $\gamma\gamma \rightarrow \pi_2 \rightarrow \pi^0\pi^0\pi^0$ [46] and $\gamma\gamma \rightarrow \pi_2 \rightarrow \pi^+\pi^-\pi^0$ [47] also see indications of a possible contribution around 1.8 GeV. (In both cases the data appear skewed towards the higher masses relative to simple Breit Wigner and PDG values.) This may be expected for $\pi_{2(D)}$ through VMD as its $\rho\omega$ coupling is predicted to be large and thereby provide a further probe for any 2D component in $\pi_2(1800)$ state. It may be possible for LEP2 to clarify this situation.

If there is indeed a second π_2 state near 1.8 GeV, it is much too light to be a radial excitation of the $\pi_2(1670)$, and may instead be a hybrid. To test this possibility we have calculated the branching fractions of a $\pi_2(1800)$ hybrid in the flux tube model, and for comparison we show the partial widths of a hypothetical 1D quarkonium $\pi_2(1800)$. These are given in Table V. (The partial widths to $a_1(1230)\eta$ and $K_1^*(1273)K$ are < 1 MeV in both models, so these modes are not displayed.)

TABLE V. Partial widths of 1D and hybrid $\pi_2(1800)$ states.

	$\rho\pi$	$\omega\rho$	$\rho_R\pi$	$b_1\pi$	$f_0\pi$	$f_1\pi$	$f_2\pi$	K^*K	total
$\pi_{2(1D)}(1800)$	162.	69.	0.	0.	1.	5.	86.	49.	372.
$\pi_{2(H)}(1800)$	8	0	5	15	1	0	50	1	80

Evidently there are very characteristic differences between hybrid and 1D (π_2) branching fractions. First, note that a large $f_2(1275)\pi$ mode is *not* distinctive; this is expected from both states. A 1D quarkonium should also couple strongly to $\rho\pi$, $\omega\rho$ and K^*K , and the total width should be about 400 MeV. In contrast, these S+S modes are weak for a hybrid; the second largest mode (after $f_2\pi$) should be $b_1\pi$, which is forbidden to quarkonium by the singlet selection rule. Clearly a study of $b_1\pi$ final states in processes that report a $\pi_2(1800)$ would be very useful as a hybrid search. Other modes are quite small, so the hybrid should be a relatively narrow state, with a total width of only about 100 MeV. In summary, the characteristic signature of a $\pi_{2(H)}(1800)$ hybrid is a strong $f_2\pi$ mode and some $b_1\pi$ but weak couplings to $\rho\pi$, $\omega\rho$ and K^*K .

C. η_2

A doubling of 2^{-+} peaks has also been reported by Crystal Barrel, in the isoscalar sector in $p\bar{p} \rightarrow (\eta\pi^0\pi^0)\pi^0$ [48]. Masses and widths of $M = 1645(14)(15)$ MeV, $\Gamma = 180^{+40}_{-21}(25)$ MeV and $M = 1875(20)(35)$ MeV, $\Gamma = 200(25)(45)$ MeV have been reported for the two 2^{-+} states. This $\eta_2(1645)$ is seen in $a_2(1318)\pi$ [49], and in view of the approximate degeneracy with the $\pi_2(1670)$ and other 1D candidates is probably the 1D_2 $n\bar{n}$ isosinglet partner of $\pi_2(1670)$. The higher-mass state $\eta_2(1875)$ has been seen only in $f_2(1275)\eta$ (only 50 MeV above threshold), and no evidence of it is found in $a_0(980)\pi$, $f_0(980)\eta$ or $f_0(1300)\eta$. The Crystal Ball Collaboration some time ago reported a 2^{-+} (or possibly 0^{-+}) at 1880 MeV, with a width of 220 MeV, decaying equally to $a_2(1318)\pi$ and $a_0(980)\pi$ [46]. These data are also consistent with a contribution from $\eta_2(1645)$. One

TABLE VI. Partial widths of 1D and hybrid $\eta_2(1875)$ states.

	$\rho\rho$	$\omega\omega$	$f_2\eta$	$a_0(1450)\pi$	$a_1\pi$	$a_2\pi$	K^*K	total
$\eta_{2(1D)}(1875)$	147.	46.	45.	1.	43.	264.	61.	607.
$\eta_{2(H)}(1875)$	0	0	20	2	0	160	10	≈ 190

expects $\gamma\gamma \rightarrow \eta_2 > \gamma\gamma \rightarrow \pi_2$, with the magnitude of the signal in $\gamma\gamma \rightarrow \eta\pi\pi$ depending on $\text{BR}(\eta_2 \rightarrow \eta\pi\pi)$. Here again LEP2 may have much to contribute.

In Table VI we compare the decay modes expected for a hybrid at 1875 MeV with 3P_0 model predictions for a hypothetical 1D_2 $\eta_2(1875)$ quarkonium. Both assignments lead to a significant $f_2\eta$ signal, and both predict a much larger $a_2\pi$ mode.

The most characteristic modes are $\rho\rho$ and $\omega\omega$, which should be very weak for a hybrid but large for a 1D quarkonium. Similar results follow for K^*K and $a_1\pi$. Clearly searches for $a_2\pi$, $\rho\rho$ and $\omega\omega$ would be most useful. The large predicted coupling to $\rho\rho$ for the $\eta_{2(1D)}$ encourages a search in $\gamma\gamma$ for this state.

D. 3D_J states

Here we consider only the 3D_3 and 3D_2 states since the 3D_1 vectors were previously discussed with the 2^3S_1 states. The 3^{--} states $\rho_3(1691)$ and $\omega_3(1667)$ are well established 3D_3 $n\bar{n}$ quarkonia, with masses as expected for 1D states and widths of about 200 MeV. The ρ_3 (Table B7) is expected to decay mainly to $\rho\rho$ (41%) and $\pi\pi$ (34%), with a somewhat weaker $\omega\pi$ mode (11%). Experimentally the decays to 4π are about 70%, of which 16(6)% is $\omega\pi$. The $\pi\pi$ branching fraction is observed to be 23.6(1.6)%. There are also KK and K^*K modes of a few percent, roughly as predicted. The total width is predicted to be 174 MeV with these parameters, consistent with observation. Thus the $\rho_3(1691)$ appears to decay approximately as predicted by the 3P_0 model, which supports the application of the model to decays of high-L states.

Its isoscalar partner $\omega_3(1667)$ is a more interesting case. Since few modes are open

and the couplings are rather weak, we predict a total width of only 69 MeV. Although this appears inconsistent with the PDG width of 168(10) MeV, this observed value is presumably broadened by the hadronic width of the ρ and b_1 in the two-body modes $\rho\pi$ and $b_1\pi$. The reported modes are $\rho\pi$ and $\omega\pi\pi$; we expect $\rho\pi$ to be dominant, with $\approx 10\%$ branches to $b_1\pi$ (the source of $\omega\pi\pi$?) and KK . The KK mode affords an opportunity to measure the actual width of the ω_3 , which may be much smaller than it appears in $\rho\pi$ and $b_1\pi$ modes.

Our results for the 3D_2 2^{--} states $\rho_2(1670)$ and $\omega_2(1670)$ are especially interesting because these are “missing mesons” in the quark model. We find that these are rather broad states, with total widths of about 300-400 MeV. The ρ_2 is predicted to have a large branching fraction of 54% to $a_2\pi$, so it should be observable in this final state or in the secondary modes $\omega\pi$ or K^*K . The ω_2 is predicted to have an even larger branching fraction of 74% to $\rho\pi$. It too couples significantly to K^*K , and may also be observable in $\omega\eta$.

VII. 1F STATES

The 1F states provide us with an opportunity to test the accuracy of the 3P_0 decay model predictions for higher quarkonium states, since the 4^{++} and $3^{+\pm}$ states expected near 2.05 GeV do not have competing assignments as glueballs or hybrids. At present only two of these states are reasonably well established, the $f_4(2044)$ and $a_4(2037)$ [14]. There is also some evidence for an $a_3(2080)$ [16].

We do not yet have experimental branching fractions for the $I=1$ 1F states. The $a_4(2037)$ is seen in KK and 3π , and the $a_3(2080)$ is reported in 3π and $\rho_3(1691)\pi$, with $\rho_3\pi$ dominant. The branching fractions of the $f_4(2044)$ are known with more accuracy; $\omega\omega$ and $\pi\pi$ are important modes, 26(6)% and 17.0(1.5)%. KK and $\eta\eta$ modes are both known, with reported branching fractions of about 0.7% and 0.2% respectively.

3P_0 predictions for the decays of these 3F_J states are given in Tables B11 and B12.

The $a_4(2050)$ is indeed expected to appear in 3π (mainly $\rho\pi$), and the dominant mode is predicted to be $\rho\omega$. This state is predicted to be rather narrower than reported. The $a_3(2080)$ is predicted to decay dominantly to $\rho_3\pi$, as is observed. The 3π mode is also predicted to be large, and to arise from both $\rho\pi$ and $f_2\pi$. The $f_4(2044)$ 3P_0 model predictions are also in qualitative agreement with experiment, in that $\pi\pi$ and $\omega\omega$ are expected to be important modes, as observed. The f_4 partial widths to pseudoscalar pairs are uniformly too large, for example $\Gamma_{f_4 \rightarrow \pi\pi}^{thy.} = 62$. MeV but $\Gamma_{f_4 \rightarrow \pi\pi}^{expt.} = 35(4)$ MeV. This decay however is G-wave, so the rate has a prefactor of $|\vec{p}_\pi/\beta|^9$; this extreme sensitivity means that a small increase of β by $\approx 10\%$, halves the decay rate and gives agreement with experiment. Thus this disagreement is quite sensitive to parameters and is probably not significant.

The predictions for branching fractions of the five missing $I=0,1$ $1F$ states suggest that several of them may easily be found by reconstructing the appropriate final states. The total widths of all except the 3F_2 states are predicted to be ~ 300 MeV, so they should be observable experimentally. The $f_3(2050)$ is predicted to couple dominantly to $a_2\pi$. In the spin-singlet 1F_3 sector, the $h_3(2050)$ should appear in $\rho\pi$ and $\rho_3(1691)\pi$, just as we found for the $a_3(2080)$. The $b_3(2050)$ should be evident in $a_2\pi$, and less strongly in $\omega_3\pi$, $\omega\pi$ and $\rho\rho$. Modes such as $a_2\pi$ are preferable because the two-body mesons are not excessively broad and they are far from threshold, so a resonance can be distinguished from a threshold effect. In some cases the amplitude structure of these final states is also characteristic; these can be determined from the results quoted in App.A.

The missing 3F_2 states may be more difficult to identify, as we predict large total widths of ≈ 600 MeV for these states. The $a_2(2050)$ couples most strongly to $b_1\pi$; $\eta_2(1645)\pi$ and $K_1^*(1273)K$ are other important modes. Its $I=0$ partner $f_2(2050)$ should be evident in $\pi_2(1670)\pi$ and will also populate $K_1^*(1273)K$ final states.

Identification of these $1F$ states and determination of their branching fractions and decay amplitudes will be a very useful contribution to the study of resonances, as it

will allow detailed tests of the usefulness of the 3P_0 model as a means for identifying quarkonium states in this crucial 2 GeV region.

VIII. SUMMARY AND EXPERIMENTAL STRATEGY

We have established that the $a_1(1700)$ is very likely a 2P radial excitation. This follows from the weak S-wave and strong D-wave in $\rho\pi$. This also establishes the natural mass scale for the 2P multiplets as ≈ 1.7 GeV. We have been unable to identify radial scalars. These are predicted to be broad, and so their non-appearance is not surprising. Conversely it raises interest in the (relatively narrow) $f_0(1500)$ and possible scalar $f_J(1710)$. We do identify some (more speculative) potential candidates for 2^{++} 2P members. We note that $\gamma\gamma$ production may help identify these radial 2P states and also clarify the nature of $f_0(1500)$ and $f_J(1710)$ [40].

The $\pi(1300)$ and $\eta(1295)$ appear to be convincing 2S states. This conclusion is based on their relative widths; the large $\rho\pi$ mode of the $\pi(1300)$ has no analog for its η counterparts. The status of the $\eta(1440)$ remains open; the mass and width suggest a dominantly $s\bar{s}$ state, but the $\gamma\rho$ mode argues against it. Studies of $\psi \rightarrow \eta(1295, 1440) + (\omega, \phi)$ and $\psi \rightarrow \gamma + (\gamma\omega, \gamma\rho, \gamma\phi)$ may identify the flavor content of these η states.

The $\rho(1465)$ and $\omega(1419)$ have masses that are consistent with radial 2S but their decays show characteristics of hybrids, as noted previously [2]. We suggest that these states may be 2S-hybrid mixtures analogous to the 3S-hybrid mixing suggested for the $c\bar{c}$ [50]. This can be tested by accurate measurement of the partial widths of these states and their vector partners at 1.6-1.7 GeV to $\pi\pi$, $\omega\pi$, and especially $h_1\pi$ and $a_1\pi$.

The 3S π is expected in the 1800 MeV mass region as is a π_H hybrid. We find that the decay patterns of these states are very different. A strong $f_0(1300)\pi$ from the hybrid contrasted with a large $\rho\omega$ mode from the 3S quarkonium is the sharpest discriminant. The VES state $\pi(1800)$ clearly exhibits this hybrid signature. It is now necessary to establish the presence of 0^{-+} in the $\rho\omega$ channel, and to see if any resonant state is present

that is distinct from the $\pi(1800)$ seen in $f_0(1300)\pi$. It is possible that there are two $\pi(\approx 1800)$ states, $q\bar{q}$ and hybrid, whose production mechanisms and decay fractions differ sufficiently so that they can be separated. We suggest that the possibility of two such $\pi(\approx 1800)$ states be allowed for in data analyses.

In the immediate future there are opportunities for $\gamma\gamma$ physics at LEP2 and at B factories. Possible strategies for isolating some of these higher quarkonia include:

- $\gamma\gamma \rightarrow 5\pi$ contains (i) $\rho\omega$ which may access the radial a_{0R} and a_{2R} near 1700 MeV and a possible $\pi_{3S}(1800)$. (ii) πb_1 which can isolate the a_{0R} if the helicity selection rule [32] is used to suppress the a_{2R} .
- $\gamma\gamma \rightarrow 4\pi$ may access the radial f_{2R} near 1700 MeV through its decay into $\rho\rho$. The 4π channel may also be searched for the $f_0(1500)$ since this state is known to have a significant branching fraction to 4π but should have a suppressed $\gamma\gamma$ coupling if it is a glueball [40].
- $\gamma\gamma \rightarrow 3\pi$ may be searched for 2^{-+} states in order to verify whether the established $\pi_2(1670)$ is accompanied by a higher $\pi_2(1800)$ in $3\pi^0$ and $\pi^+\pi^-\pi^0$. This 3π system may also be studied for evidence of one or more $\pi(1800)$ states.
- $\gamma\gamma \rightarrow \eta\pi\pi$ may access the isoscalar partners of these π_2 states.

In the near future it will be possible to study e^+e^- annihilation up to ≈ 2 GeV at DAFNE. The channels $e^+e^- \rightarrow 4\pi$ should be measured and πa_1 and πh_1 states separated in order to carry out the analysis of hybrid and radial vector components in section 3B. The isoscalar partners of the vectors also need confirmation, and final states with kaons are needed to investigate possible ω - ϕ mixing; a potential weakness of the present data analyses is that such flavor mixing is assumed to be unimportant.

In the next century there will be new opportunities at the COMPASS facility at CERN. This will enable further studies of central production and also of diffractive excitation. For the latter one may anticipate improved studies of the π excitations (such as the $\pi(1300)$ and $\pi(1800)$ states), possibly including Primakoff excitation. Judicious studies of specific

final states as discussed above may help separate 3S and hybrid states. The use of K beams will allow analogous studies of the strange counterparts of these states and may help to clarify the spectrum of quarkonia, glueballs and hybrids.

Experiments with π beams can access the following interesting channels.

- $\pi p \rightarrow (\pi f_1)p$, to confirm the D-wave dominance of $a_{1R}(1700)$ and to seek its partner a_{2R} .

- $\pi p \rightarrow (\pi f_2)p$ can access both $\pi_{2(1D)}$ and $\pi_{2(H)}$. These can be separated in $b_1\pi$; the singlet selection rule forbids this mode for $\pi_{2(1D)}$ but allows it for $\pi_{2(H)}$. $(\pi\rho)p$ can also separate $\pi_{2(1D)}$ from $\pi_{2(H)}$; $\pi_{2(1D)} \rightarrow \rho\pi$ is the dominant mode whereas $\pi_{2(H)}$ is much suppressed into S+S hadrons.

- $(\pi\pi)$, $(\pi\omega)$, $(a_1\pi)$ and $(h_1\pi)$ are important in the interpretation of the vectors between 1.4 and 1.7 GeV, which may contain large hybrid components.

- $(f_0\pi)$, $(f_2\pi)$ and $(\rho\omega)$ can all be searched for evidence of $\pi(1800)$ states.

- $\pi^- p \rightarrow (\pi\rho)^0 n$ or $(\pi\omega)^0 n$ access respectively h_{1R} and b_{1R} .

Finally, many two-body channels are predicted to couple strongly to specific 2P, 1D and 1F states, as shown in Appendix B. These include “missing mesons” such as the 3F_2 and most 2P states, and studies of these two-body final states may reveal the missing resonances. The modes $a_2\pi$, $\rho\rho$ and $b_1\pi$ are important for many of these missing states and merit careful investigation.

We reiterate that it is in general a good strategy to study decays into both S+S and S+P meson modes, as the relative couplings of these modes are usually quite distinct for hybrid versus quarkonium assignments.

ACKNOWLEDGMENTS

We would like to acknowledge useful communications with C.Amsler, D.V.Bugg, S.U.Chung, G.Condo, K.Danyo, A.Dzierba, S.Godfrey, I.Kachaev, Y.Khokhlov, A.Kirk, D.Ryabchikov and A.Zaitsev. This work was supported in part by the United States Department of Energy under contracts DE-FG02-96ER40944 at North Carolina State University and DE-AC05-96OR22464 managed by Lockheed Martin Energy Research Corp. at Oak Ridge National Laboratory. FEC is supported in part by European Community Human Capital Mobility Programme Eurodafne, Contract CHRX-CT92-0026.

-
- [1] N.Isgur, R.Kokoski and J.Paton, Phys. Rev. Lett. 54, 869 (1985).
- [2] F.E.Close and P.R.Page, Nucl. Phys. B443, 233 (1995); Phys. Rev. D52, 1706 (1995).
- [3] N.Isgur and J.Paton, Phys. Rev. D31, 2910 (1985).
- [4] T.Barnes, F.E.Close and E.S.Swanson, Phys. Rev. D52, 5242 (1995); see also C.Michael [5].
- [5] G.Bali *et al.* (UKQCD Collaboration), Phys. Lett. B309, 378 (1993); D.Weingarten, Nucl. Phys. B (Proc. Suppl.) 34, 29 (1994); C.Michael, Liverpool report LTH 370, hep-ph/9605243 (May 1996); F.E.Close and M.J.Teper, "On the lightest Scalar Glueball", RAL-96-040 / OUTP-96-35P (July 1996).
- [6] J.Sexton, A.Vaccarino and D.Weingarten, Phys. Rev. Lett. 75, 4563 (1995).
- [7] D.V.Amelin *et al.* (VES Collaboration), Phys. Lett. B356 (1995) 595.
- [8] S.U.Chung, private communication.
- [9] F.E.Close, p.1395 in Proc. XXVII International Conf. on High Energy Physics, Glasgow, (Institute of Physics, U.K., 1994, P.Bussey and I.Knowles eds.).
- [10] A.M.Zaitsev (VES Collaboration), p.1409 in Proc. XXVII International Conf. on High Energy Physics, Glasgow, (Institute of Physics, U.K., 1994, P.Bussey and I.Knowles eds.).
- [11] E.S.Ackleh, T.Barnes and E.S.Swanson, "On the Mechanism of Open-Flavor Strong Decays", ORNL-CTP-96-03, hep-ph-9604355 (April 1996), Phys. Rev. D (to appear).
- [12] A.LeYaouanc, L.Oliver, O.Pène and J.Raynal, Phys. Rev. D8, 2223 (1973); see also *ibid.*, D9, 1415 (1974); D11, 1272 (1975); L.Micu, Nucl. Phys. B10, 521 (1969).
- [13] G.Busetto and L.Oliver, Z.Phys. C20, 247 (1983); R.Kokoski and N.Isgur, Phys. Rev. D35, 907 (1987); P.Geiger and E.S.Swanson, Phys. Rev. D50, 6855 (1994); H.G.Blundell and

- S.Godfrey, Phys. Rev. D53, 3700 (1996).
- [14] Particle Data Group, Phys. Rev. D54, 1 (1996).
 - [15] G.Bellini et al., Phys. Rev. Lett. 48, 1697 (1982).
 - [16] Particle Data Group, Phys. Rev. D50, 1173 (1994).
 - [17] Yu. Prokoshkin (GAMS Collaboration), in Proc. of LEAP96, Dinkelsbühl, Germany, 27-31 August 1996.
 - [18] A.B.Clegg and A.Donnachie, Z. Phys. C62, 455 (1994).
 - [19] S.Godfrey and N.Isgur, Phys. Rev. D32, 189 (1985).
 - [20] A.Donnachie and Yu.S.Kalashnikova, Z.Phys. C59, 621 (1993).
 - [21] A.Abele *et al.* (Crystal Barrel Collaboration), “High-mass ρ -meson states from $\bar{p}d$ -annihilation at rest into $\pi^-\pi^0\pi^0p_{spectator}$ ”, Phys. Lett. B (to appear).
 - [22] VES Collaboration, “Diffractive reaction $\pi^- A \rightarrow \eta\eta\pi^- A$ study at 37 GeV/c”. (unpublished)
 - [23] T.Barnes and E.S.Swanson, in preparation.
 - [24] Y.Khokhlov, private communication
 - [25] R.M.Baltrusaitis *et al.* (MarkIII Collaboration) Phys. Rev. Lett. 55, 1723 (1985); Phys. Rev. D33, 1222 (1986).
 - [26] D.Bisello *et al.* (DM2 Collaboration) Phys. Lett. B192, 239 (1987); Phys. Rev. D39, 701 (1989).
 - [27] D.V.Bugg *et al.*, Phys. Lett. B353, 378 (1995).
 - [28] C.Amsler and F.E.Close, Phys. Lett. B353, 385 (1995); Phys. Rev. D53, 295 (1996).
 - [29] J.H.Lee *et al.*, Phys. Lett. B323, 227 (1994).
 - [30] T.Degener (Crystal Barrel Collaboration), in Proc. of LEAP96, Dinkelsbühl, Germany, 27-

31 August 1996.

- [31] G.Kernel (ARGUS), Proc. of PHOTON95 (World Scientific, 1995, eds. D.J.Miller, S.L.Cartwright and V.Khoze), pp.226-231, esp. Fig.2; E.Križnič, Doctoral thesis, University of Ljubljana (1993); E.Križnič, Proc. XXVII International Conf. on High Energy Physics, Glasgow 1994, (Institute of Physics, U.K., 1994, P.Bussey and I.Knowles eds.), p.1413.
- [32] Z.P.Li, F.E.Close and T.Barnes, Phys. Rev. D43, 2161 (1991); E.S.Ackleh, T.Barnes and F.E.Close, Phys. Rev. D46, 2257 (1992); T.Barnes, in Proc. IXth International Workshop on Photon-Photon Collisions, La Jolla, CA 22-26 March 1992 (World Scientific, 1992, D.O.Caldwell and H.P.Paar eds.).
- [33] See D.Morgan, M.R.Pennington and M.R.Whalley, J. Phys. G20, A1 (1994) for a review of $\gamma\gamma \rightarrow VV$ data.
- [34] H.Albrecht *et al.*, Zeit. Phys. C50, 1 (1991).
- [35] H.Albrecht *et al.* (ARGUS Collaboration), Phys. Lett. B374, 265 (1996).
- [36] G. M. Beladidze *et al.*, Zeit. Phys. C54, 367 (1992).
- [37] A. Adamo *et al.*, Phys. Lett. B287, 368 (1992).
- [38] B.May *et al.* (ASTERIX Collaboration), Phys. Lett. B225, 450 (1989); E.Aker *et al.* (Crystal Barrel Collaboration), Phys. Lett. B260, 249 (1991).
- [39] J.Bai *et al.* (BES Collaboration) "The Structure Analysis of the $f_J(1710)$ in the Radiative Decay $\psi \rightarrow \gamma K^+ K^-$ ", IHEP Report (July 1996).
- [40] F.E.Close, G.Farrar and Z.P.Li, "Determining the Gluonic Content of Isoscalar Mesons", RAL-96-052.
- [41] N.A.Törnqvist, Phys. Rev. Lett. 67, 556 (1991).
- [42] K.Dooley, E.S.Swanson and T.Barnes, Phys. Lett. B275, 478 (1992).

- [43] C.Daum *et al.*, Nucl. Phys. B182, 269 (1981).
- [44] G.Condo *et al.*, Phys. Rev. D43, 2787 (1991). See also Y.Eisenberg *et al.*, Phys. Rev. Lett. 23, 1322 (1969); D.Aston *et al.*, Nucl. Phys. B189, 15 (1981).
- [45] D.I.Ryabchikov (VES Collaboration), Proc. of Hadron95, Manchester, U.K., Aug. 1995.
- [46] D.Antreasyan *et al.* (Crystal Ball Collaboration), Z.Phys. C48, 561 (1990).
- [47] H.J.Behrend *et al.* (Cello Collaboration), Z.Phys. C46, 583 (1990).
- [48] D.V.Bugg *et al.*, Z.Phys. C (to appear), "Study of $p\bar{p} \rightarrow \eta\pi^0\pi^0\pi^0$ at 1200 MeV/c".
- [49] C.Amsler *et al.* (Crystal Barrel Collaboration), Z. Phys. C71, 227 (1996).
- [50] F.E.Close and P.R.Page, Physics Letters B366, 323 (1996).

APPENDIX A: A COMPILATION OF 3P_0 MODEL DECAY AMPLITUDES.

We quote results for the 3P_0 model $A \rightarrow BC$ meson decay amplitudes in terms of an invariant amplitude $\mathcal{M}_{L_{BC}S_{BC}}$, which is the $L_{BC}S_{BC}$ projection of the 3P_0 pair creation Hamiltonian matrix element divided by a momentum conserving delta function,

$$\mathcal{M}_{L_{BC}S_{BC}}^{A \rightarrow BC} = \langle J_A, L_{BC}, S_{BC} | BC \rangle \langle BC | H_I(^3P_0) | A \rangle / \delta(\vec{A} - \vec{B} - \vec{C}) . \quad (\text{A1})$$

This amplitude and the derivation of the 3P_0 matrix elements are discussed in detail in Appendix A of Ackleh *et al.* [11]. The partial widths $\Gamma_{A \rightarrow BC}$ are related to these decay amplitudes by

$$\Gamma_{A \rightarrow BC} = 2\pi \frac{P E_B E_C}{M_A} \sum_{LS} |\mathcal{M}_{LS}|^2 . \quad (\text{A2})$$

The full 3P_0 decay amplitude is the sum of two Feynman diagrams, called d_1 and d_2 (Fig.A1).

In a specified flavor channel these diagrams have flavor weight factors that multiply the spin-space matrix element. The flavor factors for all the processes considered in this paper are given in Table A1. The \mathcal{M} amplitudes listed below are for unit flavor factors, $I_{\text{flavor}}(d_1) = +1$ and $I_{\text{flavor}}(d_2) = \pm 1$, with the phase chosen so they add rather than cancel. (The cancelations are due to flavor symmetries such as G-parity.) Thus for a physical decay such as $\rho^+ \rightarrow \pi^+ \pi^0$ one should multiply the unit-flavor amplitude \mathcal{M} in A3 by $+1/\sqrt{2}$ before computing the decay width using (A2). Some states populate several decay channels, for example $f \rightarrow \pi^0 \pi^0$ as well as $\rightarrow \pi^+ \pi^-$; to sum over all channels one should multiply the width by the flavor multiplicity factor \mathcal{F} in the Table. In these flavor weights the pairs $(\pi, a), (\rho, b), (\omega, h)$ and $(f, \eta_{n\bar{n}})$ are equivalent, up to factors due to identical particles in the final state.

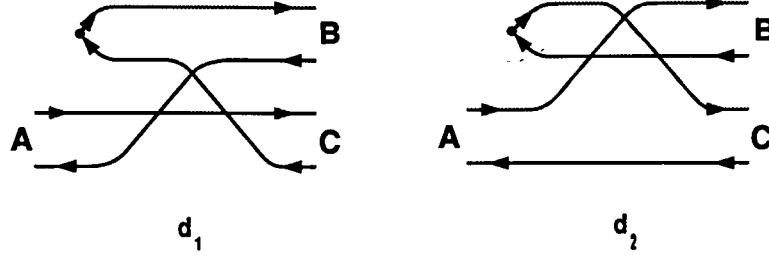


Figure A1. $q\bar{q}$ meson decay diagrams in the 3P_0 decay model.

Table A1. Flavor Weight Factors.				
Generic Decay	Subprocess	$I_{flavor}(d_1)$	$I_{flavor}(d_2)$	\mathcal{F}
$\rho \rightarrow \pi\pi$	$\rho^+ \rightarrow \pi^+\pi^0$	$+1/\sqrt{2}$	$-1/\sqrt{2}$	1
$f \rightarrow \pi\pi$	$f \rightarrow \pi^+\pi^-$	$-1/\sqrt{2}$	$-1/\sqrt{2}$	3/2
$f \rightarrow KK$	$f \rightarrow K^+K^-$	0	$-1/\sqrt{2}$	2
$a \rightarrow \rho\pi$	$a^+ \rightarrow \rho^+\pi^0$	$+1/\sqrt{2}$	$-1/\sqrt{2}$	2
$a \rightarrow KK$	$a^+ \rightarrow K^+K^0$	0	-1	1
$b \rightarrow \omega\pi$	$b^+ \rightarrow \omega\pi^+$	$+1/\sqrt{2}$	$+1/\sqrt{2}$	1
$h \rightarrow \rho\pi$	$h \rightarrow \rho^+\pi^-$	$-1/\sqrt{2}$	$-1/\sqrt{2}$	3
$K^* \rightarrow K\pi$	$K^{*+} \rightarrow K^+\pi^0$	$+1/\sqrt{2}$	0	3
$\phi \rightarrow KK$	$\phi \rightarrow K^+K^-$	+1	0	2

We take all spatial wavefunctions to be SHO forms with the same width parameter β ; as a result the \mathcal{M}_{LS} decay amplitudes are proportional to an overall Gaussian in $x = P/\beta$ times a channel-dependent polynomial $\mathcal{P}_{LS}(x)$,

$$\mathcal{M}_{LS} = \frac{\gamma}{\pi^{1/4}\beta^{1/2}} \mathcal{P}_{LS}(x) e^{-x^2/12}, \quad (\text{A3})$$

where γ is the 3P_0 pair production coupling constant [11]. To specify these amplitudes it suffices to quote the polynomial $\mathcal{P}_{LS}(x)$ for each decay channel. The complete set of 3P_0 decay amplitudes for all $q\bar{q}$ resonances with “excitation level” $\mathcal{N}_A = N_A + L_A \leq 4$ decaying

into final states with $\mathcal{N}_B \leq \mathcal{N}_A - 1$ and $C = {}^1S_0$ (and $C = {}^3S_1$ in most cases) is given below. For the relatively obscure transitions $3S \rightarrow 1D + C$, $1F \rightarrow 1P + C$, $1F \rightarrow 2P + C$ and $1F \rightarrow 1D + C$ we restrict C to 1S_0 ; this does not exclude any decays allowed by phase space.

We include a few additional amplitudes in this list. Some of these are of interest as couplings to virtual two-body states, although phase space nominally forbids the decay.

$$\boxed{1S \rightarrow 1S + 1S}$$

$$f_P = -\frac{2^5}{3^3} x \quad (\text{A4})$$

$$\boxed{{}^3S_1}$$

$$\mathcal{P}_{10}^{({}^3S_1 \rightarrow {}^1S_0 + {}^1S_0)} = f_P \quad {}^1P_1 \quad (\text{A5})$$

$$\mathcal{P}_{11}^{({}^3S_1 \rightarrow {}^3S_1 + {}^1S_0)} = -\sqrt{2} f_P \quad {}^3P_1 \quad (\text{A6})$$

$$\mathcal{P}_{LS}^{({}^3S_1 \rightarrow {}^3S_1 + {}^3S_1)} = \begin{cases} \sqrt{\frac{1}{3}} f_P & {}^1P_1 \\ 0 & {}^3P_1 \\ -\sqrt{\frac{20}{3}} f_P & {}^5P_1 \\ 0 & {}^5F_1 \end{cases} \quad (\text{A7})$$

$$\boxed{{}^1S_0}$$

$$\mathcal{P}_{LS}^{({}^1S_0 \rightarrow {}^1S_0 + {}^1S_0)} = 0 \quad (\text{A8})$$

$$\mathcal{P}_{11}^{({}^1S_0 \rightarrow {}^3S_1 + {}^1S_0)} = -\sqrt{3} f_P \quad {}^3P_1 \quad (\text{A9})$$

$$\mathcal{P}_{11}^{({}^1S_0 \rightarrow {}^3S_1 + {}^3S_1)} = \sqrt{6} f_P \quad {}^3P_1 \quad (\text{A10})$$

$$\boxed{2S \rightarrow 1S + 1S}$$

(See $1S \rightarrow 1S + 1S$ for channel coefficients.)

$$f_P = -\frac{2^{9/2}5}{3^{9/2}} x \left(1 - \frac{2}{15}x^2\right) \quad (\text{A11})$$

$$\boxed{2S \rightarrow 1P + 1S}$$

$$f_S = \frac{2^4}{3^4} \left(1 - \frac{7}{9}x^2 + \frac{2}{27}x^4\right) \quad (\text{A12})$$

$$f_D = \frac{2^{9/2}(13)}{3^6} x^2 \left(1 - \frac{2}{39}x^2\right) \quad (\text{A13})$$

$$\boxed{2^3S_1}$$

$$\mathcal{P}_{LS}^{(2^3S_1 \rightarrow ^1P_1 + ^1S_0)} = \begin{cases} f_S & ^3S_1 \\ f_D & ^3D_1 \end{cases} \quad (\text{A14})$$

$$\mathcal{P}_{LS}^{(2^3S_1 \rightarrow ^3P_1 + ^1S_0)} = \begin{cases} -\sqrt{2} f_S & ^3S_1 \\ \sqrt{\frac{1}{2}} f_D & ^3D_1 \end{cases} \quad (\text{A15})$$

$$\mathcal{P}_{22}^{(2^3S_1 \rightarrow ^3P_2 + ^1S_0)} = -\sqrt{\frac{3}{2}} f_D \quad ^5D_1 \quad (\text{A16})$$

$$\mathcal{P}_{LS}^{(2^3S_1 \rightarrow ^1P_1 + ^3S_1)} = \begin{cases} -\sqrt{\frac{1}{2}} f_D & ^3D_1 \\ \sqrt{\frac{3}{2}} f_D & ^5D_1 \end{cases} \quad (\text{A17})$$

$$\mathcal{P}_{LS}^{(2^3S_1 \rightarrow ^3P_0 + ^3S_1)} = \begin{cases} -\sqrt{3} f_S & ^3S_1 \\ 0 & ^3D_1 \end{cases} \quad (\text{A18})$$

$$\mathcal{P}_{LS}^{(2^3S_1 \rightarrow ^3P_1 + ^3S_1)} = \begin{cases} -2 f_S & ^3S_1 \\ -\frac{1}{2} f_D & ^3D_1 \\ \sqrt{\frac{3}{4}} f_D & ^5D_1 \end{cases} \quad (\text{A19})$$

$$\mathcal{P}_{LS}^{(2^3S_1 \rightarrow ^3P_2 + ^3S_1)} = \begin{cases} 0 & ^3S_1 \\ \sqrt{\frac{3}{20}} f_D & ^3D_1 \\ \frac{1}{2} f_D & ^5D_1 \\ -\sqrt{\frac{28}{5}} f_D & ^7D_1 \\ 0 & ^5G_1 \end{cases} \quad (\text{A20})$$

2^1S_0

$$\mathcal{P}_{00}^{(2^1S_0 \rightarrow ^3P_0 + ^1S_0)} = -\sqrt{3} f_S \quad ^1S_0 \quad (\text{A21})$$

$$\mathcal{P}_{22}^{(2^1S_0 \rightarrow ^3P_2 + ^1S_0)} = -\sqrt{3} f_D \quad ^5D_0 \quad (\text{A22})$$

$$\mathcal{P}_{LS}^{(2^1S_0 \rightarrow ^1P_1 + ^3S_1)} = \begin{cases} -\sqrt{3} f_S & ^1S_0 \\ -\sqrt{3} f_D & ^5D_0 \end{cases} \quad (\text{A23})$$

$$\mathcal{P}_{LS}^{(2^1S_0 \rightarrow ^3P_1 + ^3S_1)} = \begin{cases} \sqrt{6} f_S & ^1S_0 \\ -\sqrt{\frac{3}{2}} f_D & ^5D_0 \end{cases} \quad (\text{A24})$$

$$\mathcal{P}_{22}^{(2^1S_0 \rightarrow ^3P_2 + ^3S_1)} = \sqrt{\frac{9}{2}} f_D \quad ^5D_0 \quad (\text{A25})$$

$$\boxed{3S \rightarrow 1S + 1S}$$

(See $1S \rightarrow 1S + 1S$ for channel coefficients.)

$$f_P = -\frac{2^{7/2}5^{1/2}7}{3^{11/2}} x \left(1 - \frac{4}{15}x^2 + \frac{4}{315}x^4\right) \quad (\text{A26})$$

$$\boxed{3S \rightarrow 2S + 1S}$$

$$f_P = -\frac{2^4 5^{3/2}}{3^5} x \left(1 - \frac{1}{4}x^2 + \frac{1}{75}x^4 - \frac{1}{6075}x^6\right) \quad (\text{A27})$$

$$\boxed{3^3S_1}$$

$$\mathcal{P}_{10}^{(3^3S_1 \rightarrow 2^1S_0 + ^1S_0)} = f_P \quad ^1P_1 \quad (\text{A28})$$

$$\mathcal{P}_{11}^{(3^3S_1 \rightarrow 2^3S_1 + ^1S_0)} = -\sqrt{2}f_P \quad ^3P_1 \quad (\text{A29})$$

$$\mathcal{P}_{11}^{(3^3S_1 \rightarrow 2^1S_0 + ^3S_1)} = \sqrt{2}f_P \quad ^3P_1 \quad (\text{A30})$$

$$\mathcal{P}_{LS}^{(3^3S_1 \rightarrow 2^3S_1 + ^3S_1)} = \begin{cases} \sqrt{\frac{1}{3}}f_P & ^1P_1 \\ 0 & ^3P_1 \\ -\sqrt{\frac{20}{3}}f_P & ^5P_1 \\ 0 & ^5F_1 \end{cases} \quad (\text{A31})$$

$$\boxed{3^1S_0}$$

$$\mathcal{P}_{11}^{(3^1S_0 \rightarrow 2^3S_1 + ^1S_0)} = -\sqrt{3}f_P \quad ^3P_0 \quad (\text{A32})$$

$$\mathcal{P}_{11}^{(3^1S_0 \rightarrow 2^1S_0 + ^3S_1)} = -\sqrt{3}f_P \quad ^3P_0 \quad (\text{A33})$$

$$\mathcal{P}_{11}^{(3^1S_0 \rightarrow 2^3S_1 + ^3S_1)} = \sqrt{6}f_P \quad ^3P_0 \quad (\text{A34})$$

3S → 1P + 1S

(See $2S \rightarrow 1P + 1S$ for channel coefficients.)

$$f_S = \frac{2^3 5^{3/2}}{3^5} \left(1 - \frac{3}{5} x^2 + \frac{16}{225} x^4 - \frac{4}{2025} x^6 \right) \quad (\text{A35})$$

$$f_D = \frac{2^{7/2} 7^2}{3^6 5^{1/2}} x^2 \left(1 - \frac{20}{147} x^2 + \frac{4}{1323} x^4 \right) \quad (\text{A36})$$

3S → 2P + 1S

(See $2S \rightarrow 1P + 1S$ for channel coefficients.)

$$f_S = \frac{2^{5/2}}{3^4} \left(1 - \frac{47}{18} x^2 + \frac{1}{2} x^4 - \frac{8}{405} x^6 + \frac{2}{10935} x^8 \right) \quad (\text{A37})$$

$$f_D = \frac{2^{65}}{3^6} x^2 \left(1 - \frac{57}{400} x^2 + \frac{13}{2700} x^4 - \frac{1}{24300} x^6 \right) \quad (\text{A38})$$

3S → 1D + 1¹S₀

$$f_P = -\frac{2^3}{3^5} x \left(1 - \frac{23}{15} x^2 + \frac{8}{45} x^4 - \frac{4}{1215} x^6 \right) \quad (\text{A39})$$

$$f_F = -\frac{2^{5/2}(43)}{3^{11/25}} x^3 \left(1 - \frac{92}{1161} x^2 + \frac{4}{3483} x^4 \right) \quad (\text{A40})$$

3³S₁

$$\mathcal{P}_{LS}^{(3^3 S_1 \rightarrow ^1 D_2 + ^1 S_0)} = \begin{cases} f_P & ^5 P_1 \\ f_F & ^5 F_1 \end{cases} \quad (\text{A41})$$

$$\mathcal{P}_{11}^{(3^3 S_1 \rightarrow ^3 D_1 + ^1 S_0)} = \sqrt{\frac{1}{2}} f_P \quad ^3 P_1 \quad (\text{A42})$$

$$\mathcal{P}_{LS}^{(3^3 S_1 \rightarrow ^3 D_2 + ^1 S_0)} = \begin{cases} -\sqrt{\frac{3}{2}} f_P & ^5 P_1 \\ \sqrt{\frac{2}{3}} f_F & ^5 F_1 \end{cases} \quad (\text{A43})$$

$$\mathcal{P}_{33}^{(3^3 S_1 \rightarrow ^3 D_3 + ^1 S_0)} = -\sqrt{\frac{4}{3}} f_F \quad ^7 F_1 \quad (\text{A44})$$

$$\boxed{3^1\mathbf{S}_0}$$

$$\mathcal{P}_{11}^{(3^1S_0 \rightarrow ^3D_1 + ^1S_0)} = -\sqrt{3} f_P \quad ^3P_0 \quad (\text{A45})$$

$$\mathcal{P}_{33}^{(3^1S_0 \rightarrow ^3D_3 + ^1S_0)} = -\sqrt{3} f_F \quad ^7F_0 \quad (\text{A46})$$

$$\boxed{1P \rightarrow 1S + 1S}$$

$$f_S = \frac{2^5}{3^{5/2}} \left(1 - \frac{2}{9}x^2\right) \quad (\text{A47})$$

$$f_D = \frac{2^6}{3^4 5^{1/2}} x^2 \quad (\text{A48})$$

$$\boxed{{}^3P_2}$$

$$\mathcal{P}_{20}^{({}^3P_2 \rightarrow {}^1S_0 + {}^1S_0)} = f_D \quad (\text{A49})$$

$$\mathcal{P}_{21}^{({}^3P_2 \rightarrow {}^3S_1 + {}^1S_0)} = -\sqrt{\frac{3}{2}} f_D \quad (\text{A50})$$

$$\mathcal{P}_{LS}^{({}^3P_2 \rightarrow {}^3S_1 + {}^3S_1)} = \begin{cases} -\sqrt{2} f_S & {}^5S_2 \\ \sqrt{\frac{1}{3}} f_D & {}^1D_2 \\ -\sqrt{\frac{7}{3}} f_D & {}^5D_2 \end{cases} \quad (\text{A51})$$

$$\boxed{{}^3P_1}$$

$$\mathcal{P}_{LS}^{({}^3P_1 \rightarrow {}^3S_1 + {}^1S_0)} = \begin{cases} f_S & {}^3S_1 \\ -\sqrt{\frac{5}{6}} f_D & {}^3D_1 \end{cases} \quad (\text{A52})$$

$$\mathcal{P}_{LS}^{({}^3P_1 \rightarrow {}^3S_1 + {}^3S_1)} = \begin{cases} 0 & {}^3S_1 \\ 0 & {}^3D_1 \\ -\sqrt{5} f_D & {}^5D_1 \end{cases} \quad (\text{A53})$$

$$\boxed{{}^3P_0}$$

$$\mathcal{P}_{00}^{({}^3P_0 \rightarrow {}^1S_0 + {}^1S_0)} = \sqrt{\frac{3}{2}} f_S \quad {}^1S_0 \quad (\text{A54})$$

$$\mathcal{P}_{LS}^{(^3P_0 \rightarrow ^3S_1 + ^3S_1)} = \begin{cases} \sqrt{\frac{1}{2}} f_S & ^1S_0 \\ -\sqrt{\frac{20}{3}} f_D & ^5D_0 \end{cases} \quad (\text{A55})$$

$$\boxed{{}^1\mathbf{P}_1}$$

$$\mathcal{P}_{LS}^{(^1P_1 \rightarrow ^3S_1 + ^1S_0)} = \begin{cases} -\sqrt{\frac{1}{2}} f_S & ^3S_1 \\ -\sqrt{\frac{5}{3}} f_D & ^3D_1 \end{cases} \quad (\text{A56})$$

$$\mathcal{P}_{LS}^{(^1P_1 \rightarrow ^3S_1 + ^3S_1)} = \begin{cases} f_S & ^3S_1 \\ \sqrt{\frac{10}{3}} f_D & ^3D_1 \\ 0 & ^5D_1 \end{cases} \quad (\text{A57})$$

$2P \rightarrow 1S + 1S$

(See $1P \rightarrow 1S + 1S$ for channel coefficients.)

$$f_S = \frac{2^{9/2} 5^{1/2}}{3^{7/2}} \left(1 - \frac{4}{9} x^2 + \frac{4}{135} x^4 \right) \quad (\text{A58})$$

$$f_D = \frac{2^{11/2} 7}{3^5 5} x^2 \left(1 - \frac{2}{21} x^2 \right) \quad (\text{A59})$$

$2P \rightarrow 2S + 1S$

$$f_S = \frac{2^4 5^{1/2} 7}{3^5} \left(1 - \frac{1}{2} x^2 + \frac{2}{45} x^4 - \frac{2}{2835} x^6 \right) \quad (\text{A60})$$

$$f_D = \frac{2^6 (11)}{3^{11/2} 5} x^2 \left(1 - \frac{13}{132} x^2 + \frac{1}{594} x^4 \right) \quad (\text{A61})$$

2^3P_2

$$\mathcal{P}_{20}^{(2^3P_2 \rightarrow 2^1S_0 + ^1S_0)} = f_D \quad ^1D_2 \quad (\text{A62})$$

$$\mathcal{P}_{21}^{(2^3P_2 \rightarrow 2^3S_1 + ^1S_0)} = -\sqrt{\frac{3}{2}} f_D \quad ^3D_2 \quad (\text{A63})$$

$$\mathcal{P}_{21}^{(2^3P_2 \rightarrow 2^1S_0 + ^3S_1)} = +\sqrt{\frac{3}{2}} f_D \quad ^3D_2 \quad (\text{A64})$$

$$\mathcal{P}_{LS}^{(2^3P_2 \rightarrow 2^3S_1 + ^3S_1)} = \begin{cases} -\sqrt{2} f_S & ^5S_2 \\ \sqrt{\frac{1}{3}} f_D & ^1D_2 \\ 0 & ^3D_2 \\ -\sqrt{\frac{7}{3}} f_D & ^5D_2 \\ 0 & ^5G_2 \end{cases} \quad (\text{A65})$$

2^3P_1

$$\mathcal{P}_{LS}^{(2^3P_1 \rightarrow 2^3S_1 + ^1S_0)} = \begin{cases} f_S & ^3S_1 \\ -\sqrt{\frac{5}{6}} f_D & ^3D_1 \end{cases} \quad (\text{A66})$$

$$\mathcal{P}_{LS}^{(2^3P_1 \rightarrow 2^1S_0 + ^3S_1)} = \begin{cases} -f_S & ^3S_1 \\ \sqrt{\frac{5}{6}} f_D & ^3D_1 \end{cases} \quad (\text{A67})$$

$$\mathcal{P}_{22}^{(2^3P_1 \rightarrow 2^3S_1 + ^3S_1)} = -\sqrt{5} f_D \quad ^5D_1 \quad (\text{A68})$$

$$\boxed{2^3P_0}$$

$$\mathcal{P}_{00}^{(2^3P_0 \rightarrow 2^1S_0 + ^1S_0)} = \sqrt{\frac{3}{2}} f_S \quad ^1S_0 \quad (\text{A69})$$

$$\mathcal{P}_{LS}^{(2^3P_0 \rightarrow 2^3S_1 + ^3S_1)} = \begin{cases} \sqrt{\frac{1}{2}} f_S & ^1S_0 \\ -\sqrt{\frac{20}{3}} f_D & ^5D_0 \end{cases} \quad (\text{A70})$$

$$\boxed{2^1P_1}$$

$$\mathcal{P}_{LS}^{(2^1P_1 \rightarrow 2^3S_1 + ^1S_0)} = \begin{cases} -\sqrt{\frac{1}{2}} f_S & ^3S_1 \\ -\sqrt{\frac{5}{3}} f_D & ^3D_1 \end{cases} \quad (\text{A71})$$

$$\mathcal{P}_{LS}^{(2^1P_1 \rightarrow 2^1S_0 + ^3S_1)} = \begin{cases} -\sqrt{\frac{1}{2}} f_S & ^3S_1 \\ -\sqrt{\frac{5}{3}} f_D & ^3D_1 \end{cases} \quad (\text{A72})$$

$$\mathcal{P}_{LS}^{(2^1P_1 \rightarrow 2^3S_1 + ^3S_1)} = \begin{cases} f_S & ^3S_1 \\ \sqrt{\frac{10}{3}} f_D & ^3D_1 \\ 0 & ^5D_1 \end{cases} \quad (\text{A73})$$

$$\boxed{2P \rightarrow 1P + 1S}$$

$$\boxed{2^3P_2}$$

$$\mathcal{P}_{LS}^{(2^3P_2 \rightarrow ^1P_1 + ^1S_0)} = \begin{cases} -\frac{2^{9/2}(13)}{3^5 5^{1/2}} x \left(1 - \frac{8}{39}x^2 + \frac{4}{585}x^4\right) & ^3P_2 \\ -\frac{2^5}{3^{9/2} 5^{1/2}} x^3 \left(1 - \frac{2}{45}x^2\right) & ^3F_2 \end{cases} \quad (\text{A74})$$

$$\mathcal{P}_{LS}^{(2^3P_2 \rightarrow ^3P_1 + ^1S_0)} = \begin{cases} \frac{2^6}{3^4 5^{1/2}} x \left(1 - \frac{1}{4}x^2 + \frac{1}{90}x^4\right) & ^3P_2 \\ -\frac{2^{9/2}}{3^{9/2} 5^{1/2}} x^3 \left(1 - \frac{2}{45}x^2\right) & ^3F_2 \end{cases} \quad (\text{A75})$$

$$\mathcal{P}_{LS}^{(2^3P_2 \rightarrow ^3P_2 + ^1S_0)} = \begin{cases} \frac{2^{5/2} 7}{3^{9/2} 5^{1/2}} x \left(1 - \frac{1}{6}x^2 + \frac{1}{315}x^4\right) & ^5P_2 \\ \frac{2^5}{3^{9/2} 5^{1/2}} x^3 \left(1 - \frac{2}{45}x^2\right) & ^5F_2 \end{cases} \quad (\text{A76})$$

$$\mathcal{P}_{LS}^{(2^3P_2 \rightarrow ^1P_1 + ^3S_1)} = \begin{cases} -\frac{2^6}{3^4 5^{1/2}} x \left(1 - \frac{1}{4}x^2 + \frac{1}{90}x^4\right) & ^3P_2 \\ -\frac{2^{5/2} 7}{3^{9/2} 5^{1/2}} x \left(1 - \frac{1}{6}x^2 + \frac{1}{315}x^4\right) & ^5P_2 \\ \frac{2^{9/2}}{3^{9/2} 5^{1/2}} x^3 \left(1 - \frac{2}{45}x^2\right) & ^3F_2 \\ -\frac{2^5}{3^{9/2} 5^{1/2}} x^3 \left(1 - \frac{2}{45}x^2\right) & ^5F_2 \end{cases} \quad (\text{A77})$$

$$\mathcal{P}_{LS}^{(2^3P_2 \rightarrow ^3P_0 + ^3S_1)} = \begin{cases} \frac{2^{11/2} 5^{1/2}}{3^{11/2}} x \left(1 - \frac{11}{30}x^2 + \frac{1}{45}x^4\right) & ^3P_2 \\ 0 & ^3F_2 \end{cases} \quad (\text{A78})$$

$$\mathcal{P}_{LS}^{(2^3P_2 \rightarrow ^3P_1 + ^3S_1)} = \begin{cases} \frac{2^{7/2}(23)}{3^5 5^{1/2}} x \left(1 - \frac{19}{69}x^2 + \frac{14}{1035}x^4\right) & ^3P_2 \\ \frac{2^{7/2}}{3^{9/2} 5^{1/2}} x \left(1 + \frac{1}{3}x^2 - \frac{2}{45}x^4\right) & ^5P_2 \\ \frac{2^4}{3^{9/2} 5^{1/2}} x^3 \left(1 - \frac{2}{45}x^2\right) & ^3F_2 \\ -\frac{2^{9/2}}{3^{9/2} 5^{1/2}} x^3 \left(1 - \frac{2}{45}x^2\right) & ^5F_2 \end{cases} \quad (\text{A79})$$

$$\mathcal{P}_{LS}^{(2^3P_2 \rightarrow ^3P_2 + ^3S_1)} = \begin{cases} -\frac{2^{7/2}(29)}{3^{11/2} 5} x \left(1 - \frac{13}{87}x^2 + \frac{2}{1305}x^4\right) & ^3P_2 \\ \frac{2^{7/2}}{3^5 5^{1/2}} x \left(1 + \frac{1}{3}x^2 - \frac{2}{45}x^4\right) & ^5P_2 \\ \frac{2^{9/2} 7^{1/2}(41)}{3^5 5} x \left(1 - \frac{22}{123}x^2 + \frac{8}{1845}x^4\right) & ^7P_2 \\ -\frac{2^4}{3^4 5} x^3 \left(1 - \frac{2}{45}x^2\right) & ^3F_2 \\ -\frac{2^{9/2}}{3^5 5^{1/2}} x^3 \left(1 - \frac{2}{45}x^2\right) & ^5F_2 \\ \frac{2^{13/2}}{3^{9/2} 5} x^3 \left(1 - \frac{2}{45}x^2\right) & ^7F_2 \\ 0 & ^7H_2 \end{cases} \quad (\text{A80})$$

2^3P_1

$$\mathcal{P}_{11}^{(2^3P_1 \rightarrow ^1P_1 + ^1S_0)} = \frac{2^{9/2}5^{1/2}}{3^4} x \left(1 - \frac{2}{15}x^2\right) \quad ^3P_1 \quad (\text{A81})$$

$$\mathcal{P}_{10}^{(2^3P_1 \rightarrow ^3P_0 + ^1S_0)} = \frac{2^4 5^{1/2}}{3^{9/2}} x \left(1 - \frac{2}{15}x^2\right) \quad ^1P_1 \quad (\text{A82})$$

$$\mathcal{P}_{11}^{(2^3P_1 \rightarrow ^3P_1 + ^1S_0)} = \frac{2^4 5^{3/2}}{3^6} x \left(1 - \frac{17}{75}x^2 + \frac{2}{225}x^4\right) \quad ^3P_1 \quad (\text{A83})$$

$$\mathcal{P}_{LS}^{(2^3P_1 \rightarrow ^3P_2 + ^1S_0)} = \begin{cases} -\frac{2^4}{3^{5/2}} x \left(1 - \frac{5}{27}x^2 + \frac{2}{405}x^4\right) & ^5P_1 \\ \frac{2^{9/2}}{3^5} x^3 \left(1 - \frac{2}{45}x^2\right) & ^5F_1 \end{cases} \quad (\text{A84})$$

$$\mathcal{P}_{LS}^{(2^3P_1 \rightarrow ^1P_1 + ^3S_1)} = \begin{cases} -\frac{2^4 5^{1/2}}{3^{9/2}} x \left(1 - \frac{2}{15}x^2\right) & ^1P_1 \\ -\frac{2^4 5^{3/2}}{3^5} x \left(1 - \frac{17}{75}x^2 + \frac{2}{225}x^4\right) & ^3P_1 \\ \frac{2^4}{3^{5/2}} x \left(1 - \frac{5}{27}x^2 + \frac{2}{405}x^4\right) & ^5P_1 \\ -\frac{2^{9/2}}{3^5} x^3 \left(1 - \frac{2}{45}x^2\right) & ^5F_1 \end{cases} \quad (\text{A85})$$

$$\mathcal{P}_{11}^{(2^3P_1 \rightarrow ^3P_0 + ^3S_1)} = \frac{2^{9/2}5^{3/2}}{3^{11/2}} x \left(1 - \frac{17}{75}x^2 + \frac{2}{225}x^4\right) \quad ^3P_1 \quad (\text{A86})$$

$$\mathcal{P}_{LS}^{(2^3P_1 \rightarrow ^3P_1 + ^3S_1)} = \begin{cases} 0 & ^1P_1 \\ \frac{2^{9/2}5^{1/2}}{3^5} x \left(1 - \frac{11}{30}x^2 + \frac{1}{45}x^4\right) & ^3P_1 \\ \frac{2^{9/2}7}{3^{9/2}} x \left(1 - \frac{1}{6}x^2 + \frac{1}{315}x^4\right) & ^5P_1 \\ -\frac{2^4}{3^5} x^3 \left(1 - \frac{2}{45}x^2\right) & ^5F_1 \end{cases} \quad (\text{A87})$$

$$\mathcal{P}_{LS}^{(2^3P_1 \rightarrow ^3P_2 + ^3S_1)} = \begin{cases} \frac{2^{9/2}7}{3^{11/2}} x \left(1 - \frac{1}{6}x^2 + \frac{1}{315}x^4\right) & ^3P_1 \\ \frac{2^{9/2}7}{3^5} x \left(1 - \frac{1}{6}x^2 + \frac{1}{315}x^4\right) & ^5P_1 \\ -\frac{2^4}{3^{11/2}} x^3 \left(1 - \frac{2}{45}x^2\right) & ^5F_1 \\ \frac{2^{13/2}}{3^{11/2}} x^3 \left(1 - \frac{2}{45}x^2\right) & ^7F_1 \end{cases} \quad (\text{A88})$$

2^3P_0

$$\mathcal{P}_{11}^{(2^3P_0 \rightarrow ^1P_1 + ^1S_0)} = -\frac{2^{7/2}5^{1/2}(13)}{3^5} x \left(1 - \frac{8}{39}x^2 + \frac{4}{585}x^4\right) \quad ^3P_0 \quad (\text{A89})$$

$$\mathcal{P}_{11}^{(2^3P_0 \rightarrow ^3P_1 + ^1S_0)} = -\frac{2^5 5^{1/2}}{3^4} x \left(1 - \frac{2}{15}x^2\right) \quad ^3P_0 \quad (\text{A90})$$

$$\mathcal{P}_{11}^{(2^3P_0 \rightarrow ^1P_1 + ^3S_1)} = \frac{2^5 5^{1/2}}{3^4} x \left(1 - \frac{2}{15}x^2\right) \quad ^3P_0 \quad (\text{A91})$$

$$\mathcal{P}_{11}^{(2^3P_0 \rightarrow ^3P_0 + ^3S_1)} = \frac{2^{7/2}5^{1/2}(13)}{3^{11/2}} x \left(1 - \frac{8}{39}x^2 + \frac{4}{585}x^4\right) \quad ^3P_0 \quad (\text{A92})$$

$$\mathcal{P}_{11}^{(2^3P_0 \rightarrow ^3P_1 + ^3S_1)} = \frac{2^{7/2}5^{1/2}(13)}{3^5} x \left(1 - \frac{8}{39}x^2 + \frac{4}{585}x^4\right) \quad ^3P_0 \quad (\text{A93})$$

$$\mathcal{P}_{LS}^{(2^3P_0 \rightarrow ^3P_2 + ^3S_1)} = \begin{cases} -\frac{2^{7/2}(13)}{3^{11/2}} x \left(1 - \frac{8}{39}x^2 + \frac{4}{585}x^4\right) & ^3P_0 \\ \frac{2^6}{3^5} x^3 \left(1 - \frac{2}{45}x^2\right) & ^7F_0 \end{cases} \quad (\text{A94})$$

2^1P_1

$$\mathcal{P}_{11}^{(2^1P_1 \rightarrow ^1P_1 + ^1S_0)} = 0 \quad ^3P_1 \quad (\text{A95})$$

$$\mathcal{P}_{10}^{(2^1P_1 \rightarrow ^3P_0 + ^1S_0)} = \frac{2^{7/2}5^{1/2}7}{3^{11/2}} x \left(1 - \frac{4}{15}x^2 + \frac{4}{315}x^4\right) \quad ^1P_1 \quad (\text{A96})$$

$$\mathcal{P}_{10}^{(2^1P_1 \rightarrow ^3P_1 + ^1S_0)} = \frac{2^{7/2}5^{1/2}}{3^4} x \left(1 - \frac{2}{15}x^2\right) \quad ^1P_1 \quad (\text{A97})$$

$$\mathcal{P}_{LS}^{(2^1P_1 \rightarrow ^3P_2 + ^1S_0)} = \begin{cases} \frac{2^{7/2}(41)}{3^{11/2}} x \left(1 - \frac{22}{123}x^2 + \frac{8}{1845}x^4\right) & ^5P_1 \\ \frac{2^5}{3^5} x^3 \left(1 - \frac{2}{45}x^2\right) & ^5F_1 \end{cases} \quad (\text{A98})$$

$$\mathcal{P}_{LS}^{(2^1P_1 \rightarrow ^1P_1 + ^3S_1)} = \begin{cases} \frac{2^{7/2}5^{1/2}7}{3^{11/2}} x \left(1 - \frac{4}{15}x^2 + \frac{4}{315}x^4\right) & ^1P_1 \\ \frac{2^{7/2}5^{1/2}}{3^4} x \left(1 - \frac{2}{15}x^2\right) & ^3P_1 \\ \frac{2^{7/2}(41)}{3^{11/2}} x \left(1 - \frac{22}{123}x^2 + \frac{8}{1845}x^4\right) & ^5P_1 \\ \frac{2^5}{3^5} x^3 \left(1 - \frac{2}{45}x^2\right) & ^5F_1 \end{cases} \quad (\text{A99})$$

$$\mathcal{P}_{11}^{(2^1P_1 \rightarrow ^3P_0 + ^3S_1)} = \frac{2^45^{1/2}}{3^{9/2}} x \left(1 - \frac{2}{15}x^2\right) \quad ^3P_1 \quad (\text{A100})$$

$$\boxed{1D \rightarrow 1S + 1S}$$

$$f_P = \frac{2^{13/2}}{3^4} x \left(1 - \frac{2}{15} x^2\right) \quad (\text{A101})$$

$$f_F = -\frac{2^6}{3^{9/2} 5^{1/2} 7^{1/2}} x^3 \quad (\text{A102})$$

$$\boxed{{}^3D_3}$$

$$\mathcal{P}_{30}^{({}^3D_3 \rightarrow {}^1S_0 + {}^1S_0)} = f_F \quad {}^1F_3 \quad (\text{A103})$$

$$\mathcal{P}_{31}^{({}^3D_3 \rightarrow {}^3S_1 + {}^1S_0)} = -\sqrt{\frac{4}{3}} f_F \quad {}^3F_3 \quad (\text{A104})$$

$$\mathcal{P}_{LS}^{({}^3D_3 \rightarrow {}^3S_1 + {}^3S_1)} = \begin{cases} f_P & {}^5P_3 \\ \sqrt{\frac{1}{3}} f_F & {}^1F_3 \\ 0 & {}^3F_3 \\ -\sqrt{\frac{8}{5}} f_F & {}^5F_3 \\ 0 & {}^5H_3 \end{cases} \quad (\text{A105})$$

$$\boxed{{}^3D_2}$$

$$\mathcal{P}_{LS}^{({}^3D_2 \rightarrow {}^3S_1 + {}^1S_0)} = \begin{cases} -\sqrt{\frac{3}{8}} f_P & {}^3P_2 \\ -\sqrt{\frac{14}{15}} f_F & {}^3F_2 \end{cases} \quad (\text{A106})$$

$$\mathcal{P}_{LS}^{({}^3D_2 \rightarrow {}^3S_1 + {}^3S_1)} = \begin{cases} \frac{1}{2} f_P & {}^5P_2 \\ 0 & {}^3F_2 \\ -\sqrt{\frac{56}{15}} f_F & {}^5F_2 \end{cases} \quad (\text{A107})$$

$$\boxed{{}^3D_1}$$

$$\mathcal{P}_{10}^{(^3D_1 \rightarrow ^1S_0 + ^1S_0)} = -\sqrt{\frac{5}{12}} f_P \quad ^1P_1 \quad (\text{A108})$$

$$\mathcal{P}_{11}^{(^3D_1 \rightarrow ^3S_1 + ^1S_0)} = -\sqrt{\frac{5}{24}} f_P \quad ^3P_1 \quad (\text{A109})$$

$$\mathcal{P}_{LS}^{(^3D_1 \rightarrow ^3S_1 + ^3S_1)} = \begin{cases} -\frac{\sqrt{5}}{6} f_P & ^1P_1 \\ 0 & ^3P_1 \\ \frac{1}{6} f_P & ^5P_1 \\ -\sqrt{\frac{28}{5}} f_F & ^5F_1 \end{cases} \quad (\text{A110})$$

$$\boxed{{}^1D_2}$$

$$\mathcal{P}_{LS}^{(^1D_2 \rightarrow ^3S_1 + ^1S_0)} = \begin{cases} \frac{1}{2} f_P & ^3P_2 \\ -\sqrt{\frac{7}{5}} f_F & ^3F_2 \end{cases} \quad (\text{A111})$$

$$\mathcal{P}_{LS}^{(^1D_2 \rightarrow ^3S_1 + ^3S_1)} = \begin{cases} -\sqrt{\frac{1}{2}} f_P & ^3P_2 \\ 0 & ^5P_2 \\ \sqrt{\frac{14}{5}} f_F & ^3F_2 \\ 0 & ^5F_2 \end{cases} \quad (\text{A112})$$

$$\boxed{1D \rightarrow 2S + 1S}$$

$$f_P = \frac{2^6}{3^{11/2}} x \left(1 - \frac{29}{30} x^2 + \frac{1}{45} x^4 \right) \quad (\text{A113})$$

$$f_F = -\frac{2^{13/2}}{3^5 5^{1/2} 7^{1/2}} x^3 \left(1 - \frac{1}{36} x^2 \right) \quad (\text{A114})$$

$$\boxed{{}^3D_3}$$

$$\mathcal{P}_{30}^{(^3D_3 \rightarrow 2^1S_0 + ^1S_0)} = f_F \quad ^1F_3 \quad (\text{A115})$$

$$\mathcal{P}_{31}^{(^3D_3 \rightarrow 2^3S_1 + ^1S_0)} = -\sqrt{\frac{4}{3}} f_F \quad (\text{A116})$$

$$\mathcal{P}_{31}^{(^3D_3 \rightarrow 2^1S_0 + ^3S_1)} = \sqrt{\frac{4}{3}} f_F \quad (\text{A117})$$

$$\mathcal{P}_{LS}^{(^3D_3 \rightarrow 2^3S_1 + ^3S_1)} = \begin{cases} f_P & ^5P_3 \\ \sqrt{\frac{1}{3}} f_F & ^1F_3 \\ 0 & ^3F_3 \\ -\sqrt{\frac{8}{5}} f_F & ^5F_3 \\ 0 & ^5H_3 \end{cases} \quad (\text{A118})$$

$$\boxed{{}^3D_2}$$

$$\mathcal{P}_{LS}^{(^3D_2 \rightarrow 2^3S_1 + ^1S_0)} = \begin{cases} -\sqrt{\frac{3}{8}} f_P & ^3P_2 \\ -\sqrt{\frac{14}{15}} f_F & ^3F_2 \end{cases} \quad (\text{A119})$$

$$\mathcal{P}_{LS}^{(^3D_2 \rightarrow 2^1S_0 + ^3S_1)} = \begin{cases} \sqrt{\frac{3}{8}} f_P & ^3P_2 \\ \sqrt{\frac{14}{15}} f_F & ^3F_2 \end{cases} \quad (\text{A120})$$

$$\mathcal{P}_{LS}^{(^3D_2 \rightarrow 2^3S_1 + ^3S_1)} = \begin{cases} 0 & ^3P_2 \\ \frac{1}{2} f_P & ^5P_2 \\ 0 & ^3F_2 \\ -\sqrt{\frac{56}{15}} f_F & ^5F_2 \end{cases} \quad (\text{A121})$$

$$\boxed{{}^3D_1}$$

$$\mathcal{P}_{10}^{(^3D_1 \rightarrow 2^1S_0 + ^1S_0)} = -\sqrt{\frac{5}{12}} f_P \quad ^1P_1 \quad (\text{A122})$$

$$\mathcal{P}_{11}^{(^3D_1 \rightarrow 2^3S_1 + ^1S_0)} = -\sqrt{\frac{5}{24}} f_P \quad ^1P_1 \quad (\text{A123})$$

$$\mathcal{P}_{11}^{(^3D_1 \rightarrow 2^1S_0 + ^3S_1)} = \sqrt{\frac{5}{24}} f_P \quad ^1P_1 \quad (\text{A124})$$

$$\mathcal{P}_{LS}^{(^3D_1 \rightarrow 2^3S_1 + ^3S_1)} = \begin{cases} -\sqrt{\frac{5}{36}} f_P & ^1P_1 \\ 0 & ^3P_1 \\ \frac{1}{6} f_P & ^5P_1 \\ -\sqrt{\frac{28}{5}} f_F & ^5F_1 \end{cases} \quad (\text{A125})$$

$$\boxed{{}^1D_2}$$

$$\mathcal{P}_{LS}^{({}^1D_2 \rightarrow 2^3S_1 + {}^1S_0)} = \begin{cases} \frac{1}{2} f_P & {}^3P_2 \\ -\sqrt{\frac{7}{5}} f_F & {}^3F_2 \end{cases} \quad (\text{A126})$$

$$\mathcal{P}_{LS}^{({}^1D_2 \rightarrow 2^1S_0 + {}^3S_1)} = \begin{cases} \frac{1}{2} f_P & {}^3P_2 \\ -\sqrt{\frac{7}{5}} f_F & {}^3F_2 \end{cases} \quad (\text{A127})$$

$$\mathcal{P}_{LS}^{({}^1D_2 \rightarrow 2^3S_1 + {}^3S_1)} = \begin{cases} -\sqrt{\frac{1}{2}} f_P & {}^3P_2 \\ 0 & {}^5P_2 \\ \sqrt{\frac{14}{5}} f_F & {}^3F_2 \\ 0 & {}^5F_2 \end{cases} \quad (\text{A128})$$

$$\boxed{1D \rightarrow 1P + 1S}$$

$$\boxed{{}^3D_3}$$

$$\mathcal{P}_{LS}^{({}^3D_3 \rightarrow {}^1P_1 + {}^1S_0)} = \begin{cases} \frac{2^{11/2}}{3^4 5^{1/2}} x^2 \left(1 - \frac{1}{21} x^2\right) & {}^3D_3 \\ \frac{2^{13/2}}{3^{11/2} 5^{1/2} 7} x^4 & {}^3G_3 \end{cases} \quad (\text{A129})$$

$$\mathcal{P}_{LS}^{({}^3D_3 \rightarrow {}^3P_1 + {}^1S_0)} = \begin{cases} -\frac{2^6}{3^5 5^{1/2}} x^2 \left(1 - \frac{2}{21} x^2\right) & {}^3D_3 \\ \frac{2^6}{3^{11/2} 5^{1/2} 7} x^4 & {}^3G_3 \end{cases} \quad (\text{A130})$$

$$\mathcal{P}_{LS}^{({}^3D_3 \rightarrow {}^3P_2 + {}^1S_0)} = \begin{cases} -\frac{2^{15/2}}{3^5 5^{1/2}} x^2 \left(1 - \frac{1}{42} x^2\right) & {}^5D_3 \\ -\frac{2^6}{3^6 7} x^4 & {}^5G_3 \end{cases} \quad (\text{A131})$$

$$\mathcal{P}_{LS}^{(^3D_3 \rightarrow ^1P_1 + ^3S_1)} = \begin{cases} \frac{2^6}{3^5 5^{1/2}} x^2 \left(1 - \frac{2}{21} x^2\right) & ^3D_3 \\ \frac{2^{15/2}}{3^5 5^{1/2}} x^2 \left(1 - \frac{1}{42} x^2\right) & ^5D_3 \\ -\frac{2^6}{3^{11/2} 5^{1/2} 7} x^4 & ^3G_3 \\ \frac{2^6}{3^6 7} x^4 & ^5G_3 \end{cases} \quad (\text{A132})$$

$$\mathcal{P}_{21}^{(^3D_3 \rightarrow ^3P_0 + ^3S_1)} = \begin{cases} \frac{2^{11/2}}{3^{11/2} 5^{1/2}} x^2 \left(1 + \frac{1}{3} x^2\right) & ^3D_3 \\ 0 & ^3G_3 \end{cases} \quad (\text{A133})$$

$$\mathcal{P}_{LS}^{(^3D_3 \rightarrow ^3P_1 + ^3S_1)} = \begin{cases} -\frac{2^{11/2}}{3^5 5^{1/2}} x^2 \left(1 - \frac{5}{21} x^2\right) & ^3D_3 \\ -\frac{2^6}{3^5 5^{1/2}} x^2 \left(1 + \frac{1}{21} x^2\right) & ^5D_3 \\ -\frac{2^{11/2}}{3^{11/2} 5^{1/2} 7} x^4 & ^3G_3 \\ \frac{2^{11/2}}{3^6 7} x^4 & ^5G_3 \end{cases} \quad (\text{A134})$$

$$\mathcal{P}_{LS}^{(^3D_3 \rightarrow ^3P_2 + ^3S_1)} = \begin{cases} -\frac{2^7}{3^{7/2}} \left(1 - \frac{5}{18} x^2 + \frac{1}{135} x^4\right) & ^7S_3 \\ \frac{2^{11/2}}{3^{11/2}} x^2 \left(1 - \frac{1}{105} x^2\right) & ^3D_3 \\ -\frac{2^6}{3^{11/2} 5^{1/2}} x^2 \left(1 + \frac{1}{21} x^2\right) & ^5D_3 \\ -\frac{2^7}{3^5} x^2 \left(1 - \frac{4}{105} x^2\right) & ^7D_3 \\ \frac{2^{11/2}}{3^5 5^7} x^4 & ^3G_3 \\ \frac{2^{11/2}}{3^{13/2} 7} x^4 & ^5G_3 \\ -\frac{2^{15/2} (11)^{1/2}}{3^{13/2} 5^7} x^4 & ^7G_3 \end{cases} \quad (\text{A135})$$

$$\boxed{{}^3D_2}$$

$$\mathcal{P}_{21}^{(^3D_2 \rightarrow ^1P_1 + ^1S_0)} = -\frac{2^{11/2}}{3^4 5^{1/2}} x^2 \quad ^3D_2 \quad (\text{A136})$$

$$\mathcal{P}_{20}^{(^3D_2 \rightarrow ^3P_0 + ^1S_0)} = -\frac{2^5}{3^4 5^{1/2}} x^2 \quad ^1D_2 \quad (\text{A137})$$

$$\mathcal{P}_{21}^{(^3D_2 \rightarrow ^3P_1 + ^1S_0)} = -\frac{2^4 7}{3^5 5^{1/2}} x^2 \left(1 - \frac{2}{21} x^2\right) \quad ^3D_2 \quad (\text{A138})$$

$$\mathcal{P}_{LS}^{(^3D_2 \rightarrow ^3P_2 + ^1S_0)} = \begin{cases} \frac{2^{11/2}}{3^3} \left(1 - \frac{5}{18} x^2 + \frac{1}{135} x^4\right) & ^5S_2 \\ \frac{2^4 7^{1/2}}{3^5 5^{1/2}} x^2 \left(1 - \frac{2}{21} x^2\right) & ^5D_2 \\ -\frac{2^7}{3^6 5^7} x^4 & ^5G_2 \end{cases} \quad (\text{A139})$$

$$\mathcal{P}_{LS}^{(^3D_2 \rightarrow ^1P_1 + ^3S_1)} = \begin{cases} -\frac{2^{11/2}}{3^3} \left(1 - \frac{5}{18}x^2 + \frac{1}{135}x^4\right) & ^5S_2 \\ \frac{2^5}{3^4 5^{1/2}} x^2 & ^1D_2 \\ \frac{2^4 7}{3^5 5^{1/2}} x^2 \left(1 - \frac{2}{21}x^2\right) & ^3D_2 \\ -\frac{2^4 7^{1/2}}{3^5 5^{1/2}} x^2 \left(1 - \frac{2}{21}x^2\right) & ^5D_2 \\ \frac{2^7}{3^6 5} x^4 & ^5G_2 \end{cases} \quad (\text{A140})$$

$$\mathcal{P}_{21}^{(^3D_2 \rightarrow ^3P_0 + ^3S_1)} = -\frac{2^{9/2} 7}{3^{11/2} 5^{1/2}} x^2 \left(1 - \frac{2}{21}x^2\right) \quad ^3D_2 \quad (\text{A141})$$

$$\mathcal{P}_{LS}^{(^3D_2 \rightarrow ^3P_1 + ^3S_1)} = \begin{cases} -\frac{2^5}{3^3} \left(1 - \frac{5}{18}x^2 + \frac{1}{135}x^4\right) & ^5S_2 \\ -\frac{2^{7/2}}{3^5 5^{1/2}} x^2 \left(1 - \frac{2}{3}x^2\right) & ^3D_2 \\ -\frac{2^{7/2} 7^{3/2}}{3^5 5^{1/2}} x^2 \left(1 - \frac{2}{147}x^2\right) & ^5D_2 \\ \frac{2^{13/2}}{3^6 5} x^4 & ^5G_2 \end{cases} \quad (\text{A142})$$

$$\mathcal{P}_{LS}^{(^3D_2 \rightarrow ^3P_2 + ^3S_1)} = \begin{cases} -\frac{2^5}{3^{7/2}} \left(1 - \frac{5}{18}x^2 + \frac{1}{135}x^4\right) & ^5S_2 \\ -\frac{2^{7/2} 5}{3^{11/2}} x^2 \left(1 - \frac{2}{75}x^2\right) & ^3D_2 \\ -\frac{2^{7/2} 7^{3/2}}{3^{11/2} 5^{1/2}} x^2 \left(1 - \frac{2}{147}x^2\right) & ^5D_2 \\ -\frac{2^6 7^{1/2}}{3^{11/2}} x^2 \left(1 - \frac{4}{105}x^2\right) & ^7D_2 \\ \frac{2^{13/2}}{3^{13/2} 5} x^4 & ^5G_2 \\ -\frac{2^{15/2}}{3^{13/2} 5^{1/2} 7^{1/2}} x^4 & ^7G_2 \end{cases} \quad (\text{A143})$$

3D_1

$$\mathcal{P}_{LS}^{(^3D_1 \rightarrow ^1P_1 + ^1S_0)} = \begin{cases} \frac{2^6 5^{1/2}}{3^4} \left(1 - \frac{5}{18}x^2 + \frac{1}{135}x^4\right) & ^3S_1 \\ \frac{2^{15/2}}{3^6 5^{1/2}} x^2 \left(1 - \frac{1}{6}x^2\right) & ^3D_1 \end{cases} \quad (\text{A144})$$

$$\mathcal{P}_{LS}^{(^3D_1 \rightarrow ^3P_1 + ^1S_0)} = \begin{cases} \frac{2^{11/2} 5^{1/2}}{3^4} \left(1 - \frac{5}{18}x^2 + \frac{1}{135}x^4\right) & ^3S_1 \\ \frac{2^4 (23)}{3^6 5^{1/2}} x^2 \left(1 + \frac{2}{69}x^2\right) & ^3D_1 \end{cases} \quad (\text{A145})$$

$$\mathcal{P}_{22}^{(^3D_1 \rightarrow ^3P_2 + ^1S_0)} = \frac{2^4 (13)}{3^{11/2} 5^{1/2}} x^2 \left(1 - \frac{2}{39}x^2\right) \quad ^5D_1 \quad (\text{A146})$$

$$\mathcal{P}_{LS}^{(^3D_1 \rightarrow ^1P_1 + ^3S_1)} = \begin{cases} -\frac{2^{11/2}5^{1/2}}{3^4} \left(1 - \frac{5}{18}x^2 + \frac{1}{135}x^4\right) & ^3S_1 \\ -\frac{2^4(23)}{3^65^{1/2}} x^2 \left(1 + \frac{2}{69}x^2\right) & ^3D_1 \\ -\frac{2^4(13)}{3^{11/2}5^{1/2}} x^2 \left(1 - \frac{2}{39}x^2\right) & ^5D_1 \end{cases} \quad (\text{A147})$$

$$\mathcal{P}_{LS}^{(^3D_1 \rightarrow ^3P_0 + ^3S_1)} = \begin{cases} 0 & ^3S_1 \\ -\frac{2^{9/2}(13)}{3^{11/2}5^{1/2}} x^2 \left(1 - \frac{2}{39}x^2\right) & ^3D_1 \end{cases} \quad (\text{A148})$$

$$\mathcal{P}_{LS}^{(^3D_1 \rightarrow ^3P_1 + ^3S_1)} = \begin{cases} -\frac{2^55^{1/2}}{3^4} \left(1 - \frac{5}{18}x^2 + \frac{1}{135}x^4\right) & ^3S_1 \\ -\frac{2^{7/2}(47)}{3^65^{1/2}} x^2 \left(1 - \frac{10}{141}x^2\right) & ^3D_1 \\ -\frac{2^{7/2}(31)}{3^{11/2}5^{1/2}} x^2 \left(1 - \frac{2}{93}x^2\right) & ^5D_1 \end{cases} \quad (\text{A149})$$

$$\mathcal{P}_{LS}^{(^3D_1 \rightarrow ^3P_2 + ^3S_1)} = \begin{cases} \frac{2^5}{3^{7/2}} \left(1 - \frac{5}{18}x^2 + \frac{1}{135}x^4\right) & ^3S_1 \\ -\frac{2^{7/2}}{3^{11/2}} x^2 \left(1 + \frac{2}{15}x^2\right) & ^3D_1 \\ -\frac{2^{7/2}(31)}{3^65^{1/2}} x^2 \left(1 - \frac{2}{93}x^2\right) & ^5D_1 \\ -\frac{2^{11/2}7^{1/2}}{3^6} x^2 \left(1 - \frac{4}{105}x^2\right) & ^7D_1 \\ -\frac{2^{15/2}}{3^{11/2}5^{1/2}7^{1/2}} x^4 & ^7G_1 \end{cases} \quad (\text{A150})$$

$$\boxed{{}^1D_2}$$

$$\mathcal{P}_{21}^{(^1D_2 \rightarrow ^1P_1 + ^1S_0)} = 0 \quad ^3D_2 \quad (\text{A151})$$

$$\mathcal{P}_{20}^{(^1D_2 \rightarrow ^3P_0 + ^1S_0)} = -\frac{2^{13/2}}{3^{11/2}5^{1/2}} x^2 \left(1 - \frac{1}{6}x^2\right) \quad ^1D_2 \quad (\text{A152})$$

$$\mathcal{P}_{21}^{(^1D_2 \rightarrow ^3P_1 + ^1S_0)} = -\frac{2^{9/2}}{3^{7/2}5^{1/2}} x^2 \quad ^3D_2 \quad (\text{A153})$$

$$\mathcal{P}_{LS}^{(^1D_2 \rightarrow ^3P_2 + ^1S_0)} = \begin{cases} -\frac{2^6}{3^{7/2}} \left(1 - \frac{5}{18}x^2 + \frac{1}{135}x^4\right) & ^5S_2 \\ -\frac{2^{9/2}5^{1/2}7^{1/2}}{3^{11/2}} x^2 \left(1 - \frac{4}{105}x^2\right) & ^5D_2 \\ -\frac{2^{13/2}}{3^{11/2}5^{1/2}7^{1/2}} x^4 & ^5G_2 \end{cases} \quad (\text{A154})$$

$$\mathcal{P}_{LS}^{(^1D_2 \rightarrow ^1P_1 + ^3S_1)} = \begin{cases} -\frac{2^6}{3^{7/2}} \left(1 - \frac{5}{18}x^2 + \frac{1}{135}x^4\right) & ^5S_2 \\ -\frac{2^{13/2}}{3^{11/2}5^{1/2}} x^2 \left(1 - \frac{1}{6}x^2\right) & ^1D_2 \\ -\frac{2^{9/2}}{3^{7/2}5^{1/2}} x^2 & ^3D_2 \\ -\frac{2^{9/2}5^{1/2}7^{1/2}}{3^{11/2}} x^2 \left(1 - \frac{4}{105}x^2\right) & ^5D_2 \\ -\frac{2^{13/2}}{3^{11/2}5^{1/2}7^{1/2}} x^4 & ^5G_2 \end{cases} \quad (\text{A155})$$

$$\mathcal{P}_{21}^{(^1D_2 \rightarrow ^3P_0 + ^3S_1)} = -\frac{2^5}{3^4 5^{1/2}} x^2 \quad ^3D_2 \quad (\text{A156})$$

$$\mathcal{P}_{LS}^{(^1D_2 \rightarrow ^3P_1 + ^3S_1)} = \begin{cases} -\frac{2^{11/2}}{3^{7/2}} \left(1 - \frac{5}{18}x^2 + \frac{1}{135}x^4\right) & ^5S_2 \\ \frac{2^7}{3^{11/2}5^{1/2}} x^2 \left(1 - \frac{1}{6}x^2\right) & ^1D_2 \\ \frac{2^4}{3^{7/2}5^{1/2}} x^2 & ^3D_2 \\ -\frac{2^4 5^{1/2} 7^{1/2}}{3^{11/2}} x^2 \left(1 - \frac{4}{105}x^2\right) & ^5D_2 \\ -\frac{2^6}{3^{11/2}5^{1/2}7^{1/2}} x^4 & ^5G_2 \end{cases} \quad (\text{A157})$$

$$\mathcal{P}_{LS}^{(^1D_2 \rightarrow ^3P_2 + ^3S_1)} = \begin{cases} \frac{2^{11/2}}{3^3} \left(1 - \frac{5}{18}x^2 + \frac{1}{135}x^4\right) & ^5S_2 \\ \frac{2^4}{3^4} x^2 & ^3D_2 \\ \frac{2^4 5^{1/2} 7^{1/2}}{3^5} x^2 \left(1 - \frac{4}{105}x^2\right) & ^5D_2 \\ 0 & ^7D_2 \\ \frac{2^6}{3^5 5^{1/2} 7^{1/2}} x^4 & ^5G_2 \\ 0 & ^7G_2 \end{cases} \quad (\text{A158})$$

$$\boxed{1F \rightarrow 1S + 1S}$$

$$f_D = -\frac{2^{13/2}}{3^{9/2}5^{1/2}} x^2 \left(1 - \frac{2}{21}x^2\right) \quad (\text{A159})$$

$$f_G = \frac{2^{15/2}}{3^7 5^{1/2} 7^{1/2}} x^4 \quad (\text{A160})$$

$$\boxed{{}^3F_4}$$

$$\mathcal{P}_{40}^{({}^3F_4 \rightarrow {}^1S_0 + {}^1S_0)} = f_G \quad {}^1G_4 \quad (\text{A161})$$

$$\mathcal{P}_{41}^{({}^3F_4 \rightarrow {}^3S_1 + {}^1S_0)} = -\sqrt{\frac{5}{4}} f_G \quad {}^3G_4 \quad (\text{A162})$$

$$\mathcal{P}_{LS}^{({}^3F_4 \rightarrow {}^3S_1 + {}^3S_1)} = \begin{cases} f_D & {}^5D_4 \\ \sqrt{\frac{1}{3}} f_G & {}^1G_4 \\ 0 & {}^3G_4 \\ -\sqrt{\frac{55}{42}} f_G & {}^5G_4 \\ 0 & {}^5I_4 \end{cases} \quad (\text{A163})$$

$$\boxed{{}^3F_3}$$

$$\mathcal{P}_{LS}^{({}^3F_3 \rightarrow {}^3S_1 + {}^1S_0)} = \begin{cases} -\sqrt{\frac{1}{3}} f_D & {}^3D_3 \\ -\sqrt{\frac{27}{28}} f_G & {}^3G_3 \end{cases} \quad (\text{A164})$$

$$\mathcal{P}_{LS}^{({}^3F_3 \rightarrow {}^3S_1 + {}^3S_1)} = \begin{cases} 0 & {}^3D_3 \\ \sqrt{\frac{1}{3}} f_D & {}^5D_3 \\ 0 & {}^3G_3 \\ -\sqrt{\frac{45}{14}} f_G & {}^5G_3 \end{cases} \quad (\text{A165})$$

$$\boxed{{}^3F_2}$$

$$\mathcal{P}_{20}^{(^3F_2 \rightarrow ^1S_0 + ^1S_0)} = -\sqrt{\frac{7}{20}} f_D \quad ^1D_2 \quad (\text{A166})$$

$$\mathcal{P}_{21}^{(^3F_2 \rightarrow ^3S_1 + ^1S_0)} = -\sqrt{\frac{7}{30}} f_D \quad ^3D_2 \quad (\text{A167})$$

$$\mathcal{P}_{LS}^{(^3F_2 \rightarrow ^3S_1 + ^3S_1)} = \begin{cases} 0 & ^5S_2 \\ -\sqrt{\frac{7}{60}} f_D & ^1D_2 \\ 0 & ^3D_2 \\ \sqrt{\frac{1}{15}} f_D & ^5D_2 \\ -\sqrt{\frac{36}{7}} f_G & ^5G_2 \end{cases} \quad (\text{A168})$$

1F_3

$$\mathcal{P}_{LS}^{(^1F_3 \rightarrow ^3S_1 + ^1S_0)} = \begin{cases} \frac{1}{2} f_D & ^3D_3 \\ -\sqrt{\frac{9}{7}} f_G & ^3G_3 \end{cases} \quad (\text{A169})$$

$$\mathcal{P}_{LS}^{(^1F_3 \rightarrow ^3S_1 + ^3S_1)} = \begin{cases} -\sqrt{\frac{1}{2}} f_D & ^3D_3 \\ 0 & ^5D_3 \\ \sqrt{\frac{18}{7}} f_G & ^3G_3 \\ 0 & ^5G_3 \end{cases} \quad (\text{A170})$$

$1F \rightarrow 2S + 1S$

$$f_D = -\frac{2^6}{3^5 5^{1/2}} x^2 \left(1 - \frac{13}{42} x^2 + \frac{1}{189} x^4\right) \quad (\text{A171})$$

$$f_G = \frac{2^{10}}{3^{17/2} 5^{1/2} 7^{1/2}} x^4 \left(1 - \frac{1}{48} x^2\right) \quad (\text{A172})$$

3F_4

$$\mathcal{P}_{40}^{(^3F_4 \rightarrow ^2^1S_0 + ^1S_0)} = f_G \quad ^1G_4 \quad (\text{A173})$$

$$\mathcal{P}_{41}^{(^3F_4 \rightarrow ^2^3S_1 + ^1S_0)} = -\sqrt{\frac{5}{4}} f_G \quad ^3G_4 \quad (\text{A174})$$

$$\mathcal{P}_{41}^{(^3F_4 \rightarrow 2^1S_0 + ^3S_1)} = \sqrt{\frac{5}{4}} f_G \quad ^3G_4 \quad (\text{A175})$$

$$\mathcal{P}_{LS}^{(^3F_4 \rightarrow 2^3S_1 + ^3S_1)} = \begin{cases} f_D & ^5D_4 \\ \sqrt{\frac{1}{3}} f_G & ^1G_4 \\ 0 & ^3G_4 \\ -\sqrt{\frac{55}{42}} f_G & ^5G_4 \\ 0 & ^5I_4 \end{cases} \quad (\text{A176})$$

3F_3

$$\mathcal{P}_{LS}^{(^3F_3 \rightarrow 2^3S_1 + ^1S_0)} = \begin{cases} -\sqrt{\frac{1}{3}} f_D & ^3D_3 \\ -\sqrt{\frac{27}{28}} f_G & ^3G_3 \end{cases} \quad (\text{A177})$$

$$\mathcal{P}_{LS}^{(^3F_3 \rightarrow 2^1S_0 + ^3S_1)} = \begin{cases} \sqrt{\frac{1}{3}} f_D & ^3D_3 \\ \sqrt{\frac{27}{28}} f_G & ^3G_3 \end{cases} \quad (\text{A178})$$

$$\mathcal{P}_{LS}^{(^3F_3 \rightarrow 2^3S_1 + ^3S_1)} = \begin{cases} 0 & ^3D_3 \\ \sqrt{\frac{1}{3}} f_D & ^5D_3 \\ 0 & ^3G_3 \\ -\sqrt{\frac{45}{14}} f_G & ^5G_3 \end{cases} \quad (\text{A179})$$

3F_2

$$\mathcal{P}_{20}^{(^3F_2 \rightarrow 2^1S_0 + ^1S_0)} = -\sqrt{\frac{7}{20}} f_D \quad ^1D_2 \quad (\text{A180})$$

$$\mathcal{P}_{21}^{(^3F_2 \rightarrow 2^3S_1 + ^1S_0)} = -\sqrt{\frac{7}{30}} f_D \quad ^3D_2 \quad (\text{A181})$$

$$\mathcal{P}_{21}^{(^3F_2 \rightarrow 2^1S_0 + ^3S_1)} = \sqrt{\frac{7}{30}} f_D \quad ^3D_2 \quad (\text{A182})$$

$$\mathcal{P}_{LS}^{(^3F_2 \rightarrow 2^3S_1 + ^3S_1)} = \begin{cases} 0 & ^5S_2 \\ -\sqrt{\frac{7}{60}} f_D & ^1D_2 \\ 0 & ^3D_2 \\ \sqrt{\frac{1}{15}} f_D & ^5D_2 \\ -\sqrt{\frac{36}{7}} f_G & ^5G_2 \end{cases} \quad (\text{A183})$$

1F_3

$$\mathcal{P}_{LS}^{(^1F_3 \rightarrow 2^3S_1 + ^1S_0)} = \begin{cases} \frac{1}{2} f_D & ^3D_3 \\ -\sqrt{\frac{9}{7}} f_G & ^3G_3 \end{cases} \quad (\text{A184})$$

$$\mathcal{P}_{LS}^{(^1F_3 \rightarrow 2^1S_0 + ^3S_1)} = \begin{cases} \frac{1}{2} f_D & ^3D_3 \\ -\sqrt{\frac{9}{7}} f_G & ^3G_3 \end{cases} \quad (\text{A185})$$

$$\mathcal{P}_{LS}^{(^1F_3 \rightarrow 2^3S_1 + ^3S_1)} = \begin{cases} -\sqrt{\frac{1}{2}} f_D & ^3D_3 \\ 0 & ^5D_3 \\ \sqrt{\frac{18}{7}} f_G & ^3G_3 \\ 0 & ^5G_3 \end{cases} \quad (\text{A186})$$

$1F \rightarrow 3S + 1S$

(See $1F \rightarrow 2S + 1S$ for channel coefficients.)

$$f_D = \frac{2^5}{3^5 5} x^2 \left(1 + x^2 - \frac{29}{756} x^4 + \frac{1}{3402} x^6 \right) \quad (\text{A187})$$

$$f_G = \frac{2^6 7^{1/2} (11)}{3^{19/25}} x^4 \left(1 - \frac{10}{231} x^2 + \frac{1}{2772} x^4 \right) \quad (\text{A188})$$

$1F \rightarrow 1P + 1^1S_0$

3F_4

$$\mathcal{P}_{LS}^{(^3F_4 \rightarrow ^1P_1 + ^1S_0)} = \begin{cases} -\frac{2^6 5^{1/2}}{3^6 7^{1/2}} x^3 \left(1 - \frac{4}{135} x^2\right) & ^3F_4 \\ -\frac{2^7}{3^9 7^{1/2}} x^5 & ^3H_4 \end{cases} \quad (\text{A189})$$

$$\mathcal{P}_{LS}^{(^3F_4 \rightarrow ^3P_1 + ^1S_0)} = \begin{cases} \frac{2^{15/2}}{3^6 5^{1/2} 7^{1/2}} x^3 \left(1 - \frac{5}{108} x^2\right) & ^3F_4 \\ -\frac{2^{13/2}}{3^9 7^{1/2}} x^5 & ^3H_4 \end{cases} \quad (\text{A190})$$

$$\mathcal{P}_{LS}^{(^3F_4 \rightarrow ^3P_2 + ^1S_0)} = \begin{cases} \frac{2^{13/2}}{3^{11/2} 7^{1/2}} x^3 \left(1 - \frac{1}{54} x^2\right) & ^5F_4 \\ \frac{2^6}{3^{17/2} 7^{1/2}} x^5 & ^5H_4 \end{cases} \quad (\text{A191})$$

3F_3

$$\mathcal{P}_{31}^{(^3F_3 \rightarrow ^1P_1 + ^1S_0)} = \frac{2^6}{3^5 5^{1/2} 7^{1/2}} x^3 \quad ^3F_3 \quad (\text{A192})$$

$$\mathcal{P}_{30}^{(^3F_3 \rightarrow ^3P_0 + ^1S_0)} = \frac{2^6}{3^5 5^{1/2} 7^{1/2}} x^3 \quad ^1F_3 \quad (\text{A193})$$

$$\mathcal{P}_{31}^{(^3F_3 \rightarrow ^3P_1 + ^1S_0)} = \frac{2^{13/2}}{3^5 5^{1/2} 7^{1/2}} x^3 \left(1 - \frac{1}{18} x^2\right) \quad ^3F_3 \quad (\text{A194})$$

$$\mathcal{P}_{LS}^{(^3F_3 \rightarrow ^3P_2 + ^1S_0)} = \begin{cases} -\frac{2^{15/2}}{3^5} x \left(1 - \frac{1}{6} x^2 + \frac{1}{315} x^4\right) & ^5P_3 \\ \frac{2^{11/2}}{3^{15/2} 5^{1/2} 7^{1/2}} x^5 & ^5F_3 \\ \frac{2^6}{3^{15/2} 7} x^5 & ^5H_3 \end{cases} \quad (\text{A195})$$

3F_2

$$\mathcal{P}_{LS}^{(^3F_2 \rightarrow ^1P_1 + ^1S_0)} = \begin{cases} -\frac{2^{13/2} 7^{1/2}}{3^9 2^{1/2} 5^{1/2}} x \left(1 - \frac{1}{6} x^2 + \frac{1}{315} x^4\right) & ^3P_2 \\ -\frac{2^5}{3^5 5^{1/2} 7^{1/2}} x^3 \left(1 - \frac{2}{15} x^2\right) & ^3F_2 \end{cases} \quad (\text{A196})$$

$$\mathcal{P}_{LS}^{(^3F_2 \rightarrow ^3P_1 + ^1S_0)} = \begin{cases} -\frac{2^6 7^{1/2}}{3^9 2^{1/2} 5^{1/2}} x \left(1 - \frac{1}{6} x^2 + \frac{1}{315} x^4\right) & ^3P_2 \\ -\frac{2^{11/2}}{3^5 5^{1/2} 7^{1/2}} x^3 \left(1 + \frac{2}{45} x^2\right) & ^3F_2 \end{cases} \quad (\text{A197})$$

$$\mathcal{P}_{LS}^{(^3F_2 \rightarrow ^3P_2 + ^1S_0)} = \begin{cases} -\frac{2^6 7^{1/2}}{3^5 5^{1/2}} x \left(1 - \frac{1}{6} x^2 + \frac{1}{315} x^4\right) & ^5P_2 \\ -\frac{2^6}{3^5 5^{1/2} 7^{1/2}} x^3 \left(1 - \frac{2}{45} x^2\right) & ^5F_2 \end{cases} \quad (\text{A198})$$

1F_3

$$\mathcal{P}_{31}^{(^1F_3 \rightarrow ^1P_1 + ^1S_0)} = 0 \quad ^3F_3 \quad (\text{A199})$$

$$\mathcal{P}_{30}^{(^1F_3 \rightarrow ^3P_0 + ^1S_0)} = \frac{2^5}{3^{9/2} 5^{1/2} 7^{1/2}} x^3 \left(1 - \frac{2}{27} x^2\right) \quad ^1F_3 \quad (\text{A200})$$

$$\mathcal{P}_{31}^{(^1F_3 \rightarrow ^3P_1 + ^1S_0)} = \frac{2^{11/2}}{3^{9/2} 5^{1/2} 7^{1/2}} x^3 \quad ^3F_3 \quad (\text{A201})$$

$$\mathcal{P}_{LS}^{(^1F_3 \rightarrow ^3P_2 + ^1S_0)} = \begin{cases} \frac{2^{13/2}}{3^{9/2}} x \left(1 - \frac{1}{6} x^2 + \frac{1}{315} x^4\right) & ^5P_3 \\ \frac{2^{11/2}}{3^5 7^{1/2}} x^3 \left(1 - \frac{4}{135} x^2\right) & ^5F_3 \\ \frac{2^7}{3^8 7} x^5 & ^5H_3 \end{cases} \quad (\text{A202})$$

$1F \rightarrow 2P + 1^1S_0$

3F_4

$$\mathcal{P}_{LS}^{(^3F_4 \rightarrow ^2^1P_1 + ^1S_0)} = \begin{cases} -\frac{2^{11/2}(37)}{3^{7/2} 5^{1/2}} x^3 \left(1 - \frac{125}{1998} x^2 + \frac{2}{2997} x^4\right) & ^3F_4 \\ -\frac{2^{15/2} 5^{1/2}}{3^{10} 7^{1/2}} x^5 \left(1 - \frac{1}{60} x^2\right) & ^3H_4 \end{cases} \quad (\text{A203})$$

$$\mathcal{P}_{LS}^{(^3F_4 \rightarrow ^2^3P_1 + ^1S_0)} = \begin{cases} \frac{2^6(13)}{3^{7/2} 5^{1/2}} x^3 \left(1 - \frac{34}{351} x^2 + \frac{5}{4212} x^4\right) & ^3F_4 \\ -\frac{2^7 5^{1/2}}{3^{10} 7^{1/2}} x^5 \left(1 - \frac{1}{60} x^2\right) & ^3H_4 \end{cases} \quad (\text{A204})$$

$$\mathcal{P}_{LS}^{(^3F_4 \rightarrow ^2^3P_2 + ^1S_0)} = \begin{cases} \frac{2^9}{3^{13/2} 5^{1/2} 7^{1/2}} x^3 \left(1 - \frac{19}{432} x^2 + \frac{1}{2592} x^4\right) & ^5F_4 \\ \frac{2^{13/2} 5^{1/2}}{3^{19/2} 7^{1/2}} x^5 \left(1 - \frac{1}{60} x^2\right) & ^5H_4 \end{cases} \quad (\text{A205})$$

3F_3

$$\mathcal{P}_{31}^{(^3F_3 \rightarrow ^2^1P_1 + ^1S_0)} = \frac{2^{11/2}}{3^4 5^{1/2}} x^3 \left(1 - \frac{1}{54} x^2\right) \quad ^3F_3 \quad (\text{A206})$$

$$\mathcal{P}_{30}^{(^3F_3 \rightarrow ^2^3P_0 + ^1S_0)} = \frac{2^{11/2}}{3^4 5^{1/2}} x^3 \left(1 - \frac{1}{54} x^2\right) \quad ^1F_3 \quad (\text{A207})$$

$$\mathcal{P}_{31}^{(^3F_3 \rightarrow ^2^3P_1 + ^1S_0)} = \frac{2^7}{3^5 5^{1/2}} x^3 \left(1 - \frac{13}{108} x^2 + \frac{1}{648} x^4\right) \quad ^3F_3 \quad (\text{A208})$$

$$\mathcal{P}_{LS}^{(^3F_3 \rightarrow 2^3P_2 + ^1S_0)} = \begin{cases} -\frac{2^7}{3^5 5^{1/2}} x \left(1 - \frac{7}{15}x^2 + \frac{5}{252}x^4 - \frac{1}{5670}x^6\right) & ^5P_3 \\ \frac{2^6}{3^{11/2} 5^{3/2} 7^{1/2}} x^3 \left(1 + \frac{5}{27}x^2 - \frac{1}{324}x^4\right) & ^5F_3 \\ \frac{2^{13/2} 5^{1/2}}{3^{17/2} 7} x^5 \left(1 - \frac{1}{60}x^2\right) & ^5H_3 \end{cases} \quad (\text{A209})$$

3F_2

$$\mathcal{P}_{LS}^{(^3F_2 \rightarrow 2^1P_1 + ^1S_0)} = \begin{cases} -\frac{2^6 7^{1/2}}{3^9 5} x \left(1 - \frac{7}{15}x^2 + \frac{5}{252}x^4 - \frac{1}{5670}x^6\right) & ^3P_2 \\ -\frac{2^{9/2}}{3^4 5^2 7^{1/2}} x^3 \left(1 - \frac{5}{6}x^2 + \frac{1}{81}x^4\right) & ^3F_2 \end{cases} \quad (\text{A210})$$

$$\mathcal{P}_{LS}^{(^3F_2 \rightarrow 2^3P_1 + ^1S_0)} = \begin{cases} -\frac{2^{11/2} 7^{1/2}}{3^9 5} x \left(1 - \frac{7}{15}x^2 + \frac{5}{252}x^4 - \frac{1}{5670}x^6\right) & ^3P_2 \\ -\frac{2^5(19)}{3^5 5^2 7^{1/2}} x^3 \left(1 + \frac{25}{1026}x^2 - \frac{1}{1539}x^4\right) & ^3F_2 \end{cases} \quad (\text{A211})$$

$$\mathcal{P}_{LS}^{(^3F_2 \rightarrow 2^3P_2 + ^1S_0)} = \begin{cases} -\frac{2^{11/2} 7^{1/2}}{3^5 5} x \left(1 - \frac{7}{15}x^2 + \frac{5}{252}x^4 - \frac{1}{5670}x^6\right) & ^5P_2 \\ -\frac{2^{11/2}(11)}{3^5 5^2 7^{1/2}} x^3 \left(1 - \frac{5}{54}x^2 + \frac{1}{891}x^4\right) & ^5F_2 \end{cases} \quad (\text{A212})$$

1F_3

$$\mathcal{P}_{31}^{(^1F_3 \rightarrow 2^1P_1 + ^1S_0)} = 0 \quad ^3F_3 \quad (\text{A213})$$

$$\mathcal{P}_{30}^{(^1F_3 \rightarrow 2^3P_0 + ^1S_0)} = \frac{2^{9/2}}{3^{11/2} 7^{1/2}} x^3 \left(1 - \frac{49}{270}x^2 + \frac{1}{405}x^4\right) \quad ^1F_3 \quad (\text{A214})$$

$$\mathcal{P}_{31}^{(^1F_3 \rightarrow 2^3P_1 + ^1S_0)} = \frac{2^5}{3^{7/2} 5^{1/2} 7^{1/2}} x^3 \left(1 - \frac{1}{54}x^2\right) \quad ^3F_3 \quad (\text{A215})$$

$$\mathcal{P}_{LS}^{(^1F_3 \rightarrow 2^3P_2 + ^1S_0)} = \begin{cases} \frac{2^6}{3^9 5^{1/2}} x \left(1 - \frac{7}{15}x^2 + \frac{5}{252}x^4 - \frac{1}{5670}x^6\right) & ^5P_3 \\ \frac{2^5(37)}{3^6 5^{3/2} 7^{1/2}} x^3 \left(1 - \frac{125}{1998}x^2 + \frac{2}{2997}x^4\right) & ^5F_3 \\ \frac{2^{15/2} 5^{1/2}}{3^9 7} x^5 \left(1 - \frac{1}{60}x^2\right) & ^5H_3 \end{cases} \quad (\text{A216})$$

$1F \rightarrow 1D + 1^1S_0$

3F_4

$$\mathcal{P}_{LS}^{(^3F_4 \rightarrow ^1D_2 + ^1S_0)} = \begin{cases} \frac{2^7}{3^{11/2} 5^{1/2}} x^2 \left(1 - \frac{5}{42} x^2 + \frac{1}{567} x^4\right) & ^5D_4 \\ \frac{2^{11/2} 5 (11)^{1/2}}{3^{17/2} 7} x^4 \left(1 - \frac{4}{165} x^2\right) & ^5G_4 \\ \frac{2^{13/2}}{3^{19/2} 7^{1/2} (11)^{1/2}} x^6 & ^5I_4 \end{cases} \quad (\text{A217})$$

$$\mathcal{P}_{41}^{(^3F_4 \rightarrow ^3D_1 + ^1S_0)} = \frac{2^5 7^{1/2}}{3^{17/2} 5^{1/2}} x^4 \left(1 - \frac{1}{21} x^2\right) \quad ^3G_4 \quad (\text{A218})$$

$$\mathcal{P}_{LS}^{(^3F_4 \rightarrow ^3D_2 + ^1S_0)} = \begin{cases} -\frac{2^{13/2}}{3^6 5^{1/2}} x^2 \left(1 - \frac{11}{42} x^2 + \frac{5}{1134} x^4\right) & ^5D_4 \\ \frac{2^5 (11)^{1/2}}{3^8 7} x^4 \left(1 + \frac{1}{33} x^2\right) & ^5G_4 \\ \frac{2^7}{3^{10} 7^{1/2} (11)^{1/2}} x^6 & ^5I_4 \end{cases} \quad (\text{A219})$$

$$\mathcal{P}_{LS}^{(^3F_4 \rightarrow ^3D_3 + ^1S_0)} = \begin{cases} -\frac{2^{15/2}}{3^6} x^2 \left(1 - \frac{1}{21} x^2 + \frac{1}{2268} x^4\right) & ^7D_4 \\ -\frac{2^7 (11)^{1/2}}{3^7 5^{1/2} 7} x^4 \left(1 - \frac{1}{66} x^2\right) & ^7G_4 \\ -\frac{2^{11/2}}{3^{10} (11)^{1/2}} x^6 & ^7I_4 \end{cases} \quad (\text{A220})$$

3F_3

$$\mathcal{P}_{LS}^{(^3F_3 \rightarrow ^1D_2 + ^1S_0)} = \begin{cases} -\frac{2^7}{3^5 5^{1/2}} x^2 \left(1 - \frac{1}{42} x^2\right) & ^5D_3 \\ -\frac{2^{11/2}}{3^6 7} x^4 & ^5G_3 \end{cases} \quad (\text{A221})$$

$$\mathcal{P}_{LS}^{(^3F_3 \rightarrow ^3D_1 + ^1S_0)} = \begin{cases} -\frac{2^8}{3^{11/2} 5} x^2 \left(1 - \frac{2}{21} x^2 + \frac{1}{756} x^4\right) & ^3D_3 \\ -\frac{2^5 (11)}{3^7 5 7} x^4 \left(1 + \frac{1}{33} x^2\right) & ^3G_3 \end{cases} \quad (\text{A222})$$

$$\mathcal{P}_{LS}^{(^3F_3 \rightarrow ^3D_2 + ^1S_0)} = \begin{cases} -\frac{2^{13/2}}{3^{11/2} 5^{1/2}} x^2 \left(1 - \frac{1}{6} x^2 + \frac{1}{378} x^4\right) & ^5D_3 \\ -\frac{2^5}{3^{15/2}} x^4 \left(1 - \frac{1}{21} x^2\right) & ^5G_3 \end{cases} \quad (\text{A223})$$

$$\mathcal{P}_{LS}^{(^3F_3 \rightarrow ^3D_3 + ^1S_0)} = \begin{cases} \frac{2^{15/2}}{3^{9/2}} \left(1 - \frac{1}{3} x^2 + \frac{1}{60} x^4 - \frac{1}{5670} x^6\right) & ^7S_3 \\ \frac{2^{15/2}}{3^5 5} x^2 \left(1 - \frac{2}{21} x^2 + \frac{1}{756} x^4\right) & ^7D_3 \\ -\frac{2^6 (11)^{1/2}}{3^{15/2} 5 7} x^4 \left(1 + \frac{1}{33} x^2\right) & ^7G_3 \\ -\frac{2^{11/2}}{3^8 7 (11)^{1/2}} x^6 & ^7I_3 \end{cases} \quad (\text{A224})$$

3F_2

$$\mathcal{P}_{LS}^{(^3F_2 \rightarrow ^1D_2 + ^1S_0)} = \begin{cases} \frac{2^{13/2} 7^{1/2}}{3^4 5^{1/2}} \left(1 - \frac{1}{3}x^2 + \frac{1}{60}x^4 - \frac{1}{5670}x^6\right) & ^5S_2 \\ \frac{2^6}{3^4 5} x^2 \left(1 - \frac{5}{42}x^2 + \frac{1}{567}x^4\right) & ^5D_2 \\ \frac{2^5}{3^5 5^{3/2} 7} x^4 \left(1 - \frac{2}{9}x^2\right) & ^5G_2 \end{cases} \quad (\text{A225})$$

$$\mathcal{P}_{21}^{(^3F_2 \rightarrow ^3D_1 + ^1S_0)} = \frac{2^{11/2} 7^{1/2}}{3^{11/2} 5^{1/2}} x^2 \left(1 + \frac{1}{30}x^2 - \frac{1}{945}x^4\right) \quad ^3D_2 \quad (\text{A226})$$

$$\mathcal{P}_{LS}^{(^3F_2 \rightarrow ^3D_2 + ^1S_0)} = \begin{cases} \frac{2^7 7^{1/2}}{3^9 5^{1/2}} \left(1 - \frac{1}{3}x^2 + \frac{1}{60}x^4 - \frac{1}{5670}x^6\right) & ^5S_2 \\ \frac{2^{11/2} (11)}{3^{11/2} 5} x^2 \left(1 - \frac{23}{462}x^2 + \frac{1}{2079}x^4\right) & ^5D_2 \\ \frac{2^{15/2} (11)}{3^{15/2} 5^{3/2} 7} x^4 \left(1 + \frac{1}{33}x^2\right) & ^5G_2 \end{cases} \quad (\text{A227})$$

$$\mathcal{P}_{LS}^{(^3F_2 \rightarrow ^3D_3 + ^1S_0)} = \begin{cases} \frac{2^7}{3^{11/2} 5^{1/2}} x^2 \left(1 - \frac{17}{210}x^2 + \frac{1}{945}x^4\right) & ^7D_2 \\ \frac{2^{11/2} (23)}{3^{15/2} 5^7} x^4 \left(1 - \frac{2}{69}x^2\right) & ^7G_2 \end{cases} \quad (\text{A228})$$

1F_3

$$\mathcal{P}_{LS}^{(^1F_3 \rightarrow ^1D_2 + ^1S_0)} = \begin{cases} 0 & ^5D_3 \\ 0 & ^5G_3 \end{cases} \quad (\text{A229})$$

$$\mathcal{P}_{LS}^{(^1F_3 \rightarrow ^3D_1 + ^1S_0)} = \begin{cases} -\frac{2^6}{3^5 5} x^2 \left(1 - \frac{13}{42}x^2 + \frac{1}{189}x^4\right) & ^3D_3 \\ -\frac{2^5}{3^{15/2} 5^7} x^4 \left(1 - \frac{4}{3}x^2\right) & ^3G_3 \end{cases} \quad (\text{A230})$$

$$\mathcal{P}_{LS}^{(^1F_3 \rightarrow ^3D_2 + ^1S_0)} = \begin{cases} -\frac{2^{13/2}}{3^5 5^{1/2}} x^2 \left(1 - \frac{1}{42}x^2\right) & ^5D_3 \\ -\frac{2^5}{3^6 7} x^4 & ^5G_3 \end{cases} \quad (\text{A231})$$

$$\mathcal{P}_{LS}^{(^1F_3 \rightarrow ^3D_3 + ^1S_0)} = \begin{cases} -\frac{2^{13/2}}{3^4} \left(1 - \frac{1}{3}x^2 + \frac{1}{60}x^4 - \frac{1}{5670}x^6\right) & ^7S_3 \\ -\frac{2^{15/2}}{3^9 5} x^2 \left(1 - \frac{1}{14}x^2 + \frac{1}{1134}x^4\right) & ^7D_3 \\ -\frac{2^5 (11)^{1/2}}{3^5 5^7} x^4 \left(1 - \frac{2}{99}x^2\right) & ^7G_3 \\ -\frac{2^{13/2}}{3^{17/2} 7 (11)^{1/2}} x^6 & ^7I_3 \end{cases} \quad (\text{A232})$$

APPENDIX B: NUMERICAL DECAY RATES.

In this appendix we quote numerical values for partial widths predicted by the 3P_0 model. The masses used are experimental values of well established candidates, usually taken from the 1996 PDG, otherwise we used an approximate multiplet mass. These are 1700 MeV (2P), 1670 MeV (1D), 2050 MeV (1F), and 1900 MeV and 1800 MeV respectively for the 3^3S_1 and 3^1S_0 . The lighter meson masses assumed are $m_\pi = 138$ MeV, $m_K = 496$ MeV, $m_\rho = 770$ MeV, $m_\omega = 782$ MeV and $m_{K^*} = 894$ MeV. For other states we used the 1996 PDG masses except for the broad f_0 , which we left at 1300 MeV.

Although we found optimum parameters near $\gamma = 0.5$ and $\beta = 0.4$ GeV in a fit to light 1S and 1P decays, these parameters lead to moderate overestimates of the widths of the well established higher-L states $\pi_2(1670)$ and $f_4(2044)$; with this β a value closer to $\gamma = 0.4$ is preferred. Consequently we quote widths for all these higher quarkonia with the parameters

$$(\gamma, \beta) = (0.4, 0.4 \text{ GeV}) . \quad (\text{B1})$$

The tables are largely self explanatory. Except in a few cases the states are specified uniquely by their labels. The exceptions include the $|\eta(547)\rangle$ and $|\eta'(958)\rangle$, which we take to be the usual $1/\sqrt{2}$ combinations of $|n\bar{n}\rangle$ and $|s\bar{s}\rangle$ basis states. We assume that the $|\eta(1295)\rangle$ and $|\eta_2(1645)\rangle$ are pure $|n\bar{n}\rangle$ states. The strange mesons $K_1(1273)$ and $K_1(1402)$ are taken to be the linear combinations

$$|K_1(1273)\rangle = \sqrt{\frac{2}{3}} |^1P_1\rangle + \sqrt{\frac{1}{3}} |^3P_1\rangle \quad (\text{B2})$$

and

$$|K_1(1402)\rangle = -\sqrt{\frac{1}{3}} |^1P_1\rangle + \sqrt{\frac{2}{3}} |^3P_1\rangle . \quad (\text{B3})$$

This gives a zero S-wave $K_1(1273) \rightarrow K^*\pi$ coupling; experimentally D/S = 1.0(0.7), and the small partial width implies a small S-wave amplitude. The orthogonal state $K_1(1402)$

(B3) is predicted to have a D/S ratio of $+0.049$ in $K^*\pi$, quite close to the experimental $D/S = +0.04(1)$. The large $K_1(1273) \rightarrow K\rho$ mode is not predicted and is possibly due to a virtual intermediate state such as $K_0^*(1429)\pi$ followed by a final-state interaction.

The tables give partial widths for all nonstrange 2S, 3S, 2P, 1D and 1F quarkonia to all two-body modes allowed by phase space, rounded to the nearest MeV. The predictions of the dominant modes of the “missing states” in the quark model, such as the 2^{--} states and most of the 1F states, are especially interesting. If the 3P_0 model has even moderate accuracy these tables should be very useful in searches for these states.

Table B1. Partial widths of 2^3S_1 states (MeV).			
Mode	$\rho(1465)$	Mode	$\omega(1419)$
(1S)²			
$\pi \pi$	74.		
$\omega \pi$	122.	$\rho \pi$	328.
$\rho \eta$	25.	$\omega \eta$	12.
(2S)(1S)			
$\pi(1300) \pi$	0.		
(1P)(1S)			
$h_1(1170) \pi$	1.	$b_1(1231) \pi$	1.
$a_1(1230) \pi$	3.		
$a_2(1318) \pi$	0.		
(1S)² strange			
$K K$	35.		31.
$K^* K$	19.		5.
total			
$\sum_i \Gamma_i$	279.		378.
Γ_{expt}	310(60)		174(59)

Table B2. Partial widths of 2^1S_0 states (MeV).			
Mode	$\pi(1300)$	Mode	$\eta(1295)$
(1S)²			
$\pi \rho$	209.	none open	
total			
$\sum_i \Gamma_i$	209.		0.
Γ_{expt}	200 - 600		53(6)

Table B3. Partial widths of 3^3S_1 states (MeV).			
Mode	$\rho(1900)$	Mode	$\omega(1900)$
(1S)²			
$\pi \pi$	1.		
$\omega \pi$	5.	$\rho \pi$	14.
$\rho \eta$	8.	$\omega \eta$	8.
$\rho \eta'$	11.	$\omega \eta'$	10.
$\rho \rho$	92.		
(2S)(1S)			
$\pi(1300) \pi$	70.		
$\omega(1419) \pi$	50.	$\rho(1465) \pi$	121.
(1P)(1S)			
$h_1(1170) \pi$	32.	$b_1(1231) \pi$	75.
$b_1(1231) \eta$	4.	$h_1(1170) \eta$	6.
$a_1(1230) \pi$	26.		
$a_2(1318) \pi$	46.		
(2P)(1S)			
$h_1(1700) \pi$	0.	$b_1(1700) \pi$	0.
$a_1(1700) \pi$	0.		
$a_2(1700) \pi$	0.		
(1D)(1S)			
$\pi_2(1670) \pi$	0.		
$\omega_1(1649) \pi$	0.	$\rho_1(1700) \pi$	0.
$\omega_2(1670) \pi$	0.	$\rho_2(1670) \pi$	0.
$\omega_3(1667) \pi$	0.	$\rho_3(1691) \pi$	0.

Table B3 (cont.) Partial widths of 3^3S_1 states (MeV).			
Mode	$\rho(1900)$	Mode	$\omega(1900)$
(1S)² strange			
$K K$	1.		1.
$K^* K$	21.		21.
$K^* K^*$	27.		27.
(1P)(1S) strange			
$K_1^*(1273) K$	5.		5.
$K_1^*(1402) K$	4.		4.
total			
$\sum_i \Gamma_i$	403.		292.

Table B4. Partial widths of 3^1S_0 states (MeV).			
Mode	$\pi(1800)$	Mode	$\eta(1800)$
(1S)²			
$\pi \rho$	31.		
$\rho \omega$	73.	$\rho \rho$	112.
		$\omega \omega$	36.
(2S)(1S)			
$\rho(1465) \pi$	53.		
(1P)(1S)			
$f_0(1300) \pi$	7.	$a_0(1450) \pi$	30.
$f_2(1275) \pi$	28.	$a_2(1318) \pi$	61.
(1S)² strange			
$K^* K$	36.		36.
total			
$\sum_i \Gamma_i$	228.		275.
Γ_{expt}	212(37)		

Table B5. Partial widths of $2^3P_J a_J$ states (MeV).			
Mode	$a_2(1700)$	$a_1(1700)$	$a_0(1700)$
(1S)²			
$\eta \pi$	23.		5.
$\eta' \pi$	10.		5.
$\rho \pi$	104.	58.	
$\omega \rho$	109.	15.	46.
(2S)(1S)			
$\eta(1295) \pi$	3.		43.
$\rho(1465) \pi$	0.	41.	
(1P)(1S)			
$b_1(1231) \pi$	28.	41.	165.
$f_0(1300) \pi$		2.	
$f_1(1282) \pi$	4.	18.	30.
$f_2(1275) \pi$	20.	39.	
(1S)² strange			
$K K$	20.		0.
$K^* K$	17.	33.	
total			
$\sum_i \Gamma_i$	336.	246.	293.

Table B6. Partial widths of $2^3P_J f_J$ states (MeV).			
Mode	$f_2(1700)$	$f_1(1700)$	$f_0(1700)$
(1S)²			
$\pi \pi$	81.		47.
$\eta \eta$	4.		0.
$\eta \eta'$	1.		16.
$\rho \rho$	159.	27.	72.
$\omega \omega$	56.	6.	22.
(2S)(1S)			
$\pi(1300) \pi$	8.		130.
(1P)(1S)			
$a_0(1450) \pi$		1.	
$a_1(1230) \pi$	16.	70.	122.
$a_2(1318) \pi$	43.	86.	
(1S)² strange			
$K K$	20.		0.
$K^* K$	17.	33.	
total			
$\sum_i \Gamma_i$	405.	224.	409.

Table B7. Partial widths of 2^1P_1 b_1 and h_1 states (MeV).			
Mode	$b_1(1700)$	Mode	$h_1(1700)$
(1S)²			
$\omega \pi$	56.	$\rho \pi$	173.
$\rho \eta$	18.	$\omega \eta$	17.
$\rho \rho$	60.		
(2S)(1S)			
$\omega(1419) \pi$	13.	$\rho(1465) \pi$	31.
(1P)(1S)			
$h_1(1170) \pi$	0.	$b_1(1231) \pi$	0.
$a_0(1450) \pi$	2.		
$a_1(1230) \pi$	10.		
$a_2(1318) \pi$	67.		
(1S)² strange			
$K^* K$	30.		30.
total			
$\sum_i \Gamma_i$	257.		252.

Table B8. Partial widths of $^3D_J \rho_J$ states (MeV).			
Mode	$\rho_3(1691)$	$\rho_2(1670)$	$\rho_1(1700)$
(1S)²			
$\pi \pi$	59.		48.
$\omega \pi$	19.	73.	35.
$\rho \eta$	2.	28.	16.
$\rho \rho$	71.	15.	14.
(2S)(1S)			
$\pi(1300) \pi$	0.		0.
$\omega(1419) \pi$	0.	0.	0.
(1P)(1S)			
$h_1(1170) \pi$	6.	5.	124.
$a_0(1450) \pi$		0.	
$a_1(1230) \pi$	1.	3.	134.
$a_2(1318) \pi$	4.	201.	2.
(1S)² strange			
$K K$	9.		36.
$K^* K$	2.	44.	26.
total			
$\sum_i \Gamma_i$	174.	369.	435.
Γ_{expt}	215(20)		235(50)

Table B9. Partial widths of $^3D_J \omega_J$ states (MeV).			
Mode	$\omega_3(1667)$	$\omega_2(1670)$	$\omega_1(1649)$
(1S)²			
$\rho \pi$	50.	221.	101.
$\omega \eta$	2.	27.	13.
(2S)(1S)			
$\rho(1465) \pi$	0.	0.	0.
(1P)(1S)			
$b_1(1231) \pi$	7.	8.	371.
(1S)² strange			
$K K$	8.		35.
$K^* K$	2.	44.	21.
total			
$\sum_i \Gamma_i$	69.	300.	542.
Γ_{expt}	168(10)		220(35)

Table B10. Partial widths of 1D_2 π_2 and η_2 states (MeV).			
Mode	$\pi_2(1670)$	Mode	$\eta_2(1645)$
(1S)²			
$\rho \pi$	118.	$\rho \rho$	33.
$\omega \rho$	41.	$\omega \omega$	8.
(2S)(1S)			
$\rho(1465) \pi$	0..		
(1P)(1S)			
$b_1(1231) \pi$	0.		
$f_0(1300) \pi$	0.	$a_0(1450) \pi$	0.
$f_1(1282) \pi$	1.	$a_1(1230) \pi$	5.
$f_2(1275) \pi$	75.	$a_2(1318) \pi$	189.
(1S)² strange			
$K^* K$	30.		26.
total			
$\sum_i \Gamma_i$	250.		261.
Γ_{expt}	258(18)		$180^{+40}_{-21}(25)$

Table B11. Partial widths of $^3F_J a_J$ states (MeV).			
Mode	$a_4(2037)$	$a_3(2080)$	$a_2(2050)$
(1S)²			
$\eta \pi$	12.		13.
$\eta' \pi$	3.		13.
$\rho \pi$	33.	86.	37.
$\omega \rho$	54.	28.	19.
(2S)(1S)			
$\eta(1295) \pi$	1.		0.
$\pi(1300) \eta$	0.		0.
$\rho(1465) \pi$	0.	1.	0.
(1P)(1S)			
$b_1(1231) \pi$	20.	12.	140.
$f_0(1300) \pi$		4.	
$f_1(1282) \pi$	2.	6.	36.
$f_2(1275) \pi$	10.	67.	14.
$a_0(1450) \eta$		0.	
$a_1(1230) \eta$	0.	1.	16.
$a_2(1318) \eta$	0.	24.	4.
$h_1(1170) \rho$	0.	40.	21.
$b_1(1231) \omega$	0.	17.	5.
(2P)(1S)			
$b_1(1700) \pi$	0.	0.	2.
$f_0(1700) \pi$		0.	
$f_1(1700) \pi$	0.	0.	0.
$f_2(1700) \pi$	0.	1.	0.

Table B11 (cont.) Partial widths of 3F_J a_J states.			
Mode	$a_4(2037)$	$a_3(2080)$	$a_2(2050)$
(1D)(1S)			
$\eta_2(1645) \pi$	0.	3.	67.
$\rho_1(1700) \pi$	0.	1.	1.
$\rho_2(1670) \pi$	0.	1.	89.
$\rho_3(1691) \pi$	2.	127.	1.
(1S)² strange			
$K K$	8.		14.
$K^* K$	4.	28.	15.
$K^* K^*$	9.	5.	2.
(1P)(1S) strange			
$K_0^*(1429) K$		0.	
$K_1^*(1273) K$	0.	3.	91.
$K_1^*(1402) K$	0.	0.	0.
$K_2^*(1429) K$	0.	31.	4.
total			
$\sum_i \Gamma_i$	161.	483.	606.
Γ_{expt}	427(120)	340(80)	

Table B12. Partial widths of $^3F_J f_J$ states (MeV).			
Mode	$f_4(2044)$	$f_3(2050)$	$f_2(2050)$
(1S)²			
$\pi \pi$	62.		34.
$\eta \eta$	2.		4.
$\eta \eta'$	0.		5.
$\eta' \eta'$	0.		0.
$\rho \rho$	86.	37.	31.
$\omega \omega$	27.	11.	9.
(2S)(1S)			
$\pi(1300) \pi$	2.		1.
(3S)(1S)			
$\pi(1800) \pi$	0.		0.
(1P)(1S)			
$a_0(1450) \pi$		2.	
$a_1(1230) \pi$	9.	20.	113.
$a_2(1318) \pi$	22.	192.	40.
$f_0(1300) \eta$		0.	
$f_1(1282) \eta$	0.	0.	13.
$f_2(1275) \eta$	1.	25.	5.
(2P)(1S)			
$a_0(1700) \pi$		0.	
$a_1(1700) \pi$	0.	0.	1.
$a_2(1700) \pi$	0.	3.	0.

Table B12 (cont.) Partial widths of 3F_J f_J states.			
Mode	$f_4(2044)$	$f_3(2050)$	$f_2(2050)$
(1D)(1S)			
$\pi_2(1670) \pi$	1.	4.	197.
(1S)² strange			
$K K$	9.		14.
$K^* K$	5.	26.	15.
$K^* K^*$	10.	4.	2.
(1P)(1S) strange			
$K_0^*(1429) K$		0.	
$K_1^*(1273) K$	0.	2.	91.
$K_1^*(1402) K$	0.	0.	0.
$K_2^*(1429) K$	0.	23.	4.
total			
$\sum_i \Gamma_i$	237.	350.	579.
Γ_{expt}	208(13)		

Table B13. Partial widths of 1F_3 b_3 and h_3 states (MeV).			
Mode	$b_3(2050)$	Mode	$h_3(2050)$
(1S)²			
$\omega \pi$	37.	$\rho \pi$	115.
$\rho \eta$	13.	$\omega \eta$	13.
$\rho \eta'$	4.	$\omega \eta'$	4.
$\rho \rho$	33.		
(2S)(1S)			
$\omega(1419) \pi$	1.	$\rho(1465) \pi$	1.
$\rho(1465) \eta$	0.	$\omega(1419) \eta$	0.
(1P)(1S)			
$h_1(1170) \pi$	0.	$b_1(1231) \pi$	0.
$b_1(1231) \eta$	0.	$h_1(1170) \eta$	0.
$a_0(1450) \pi$	1.		
$a_1(1230) \pi$	14.		
$a_2(1318) \pi$	107.		
$a_1(1230) \omega$	3.	$a_1(1230) \rho$	12.
(2P)(1S)			
$h_1(1700) \pi$	0.	$b_1(1700) \pi$	0.
$a_0(1700) \pi$	0.		
$a_1(1700) \pi$	0.		
$a_2(1700) \pi$	1.		

Table B13 (cont.) Partial widths of 1F_3 b_3 and h_3 states (MeV).			
Mode	$b_3(2050)$	Mode	$h_3(2050)$
(1D)(1S)			
$\pi_2(1670) \pi$	0.		
$\omega_1(1700) \pi$	0.	$\rho_1(1700) \pi$	0.
$\omega_2(1670) \pi$	1.	$\rho_2(1670) \pi$	2.
$\omega_3(1667) \pi$	48.	$\rho_3(1691) \pi$	138.
(1S)² strange			
$K^* K$	22.		22.
$K^* K^*$	5.		5.
(1P)(1S) strange			
$K_0^*(1429) K$	0.		0.
$K_1^*(1273) K$	0.		0.
$K_1^*(1402) K$	0.		0.
$K_2^*(1429) K$	17.		17.
total			
$\sum_i \Gamma_i$	308.		330.